

AD-A187 037

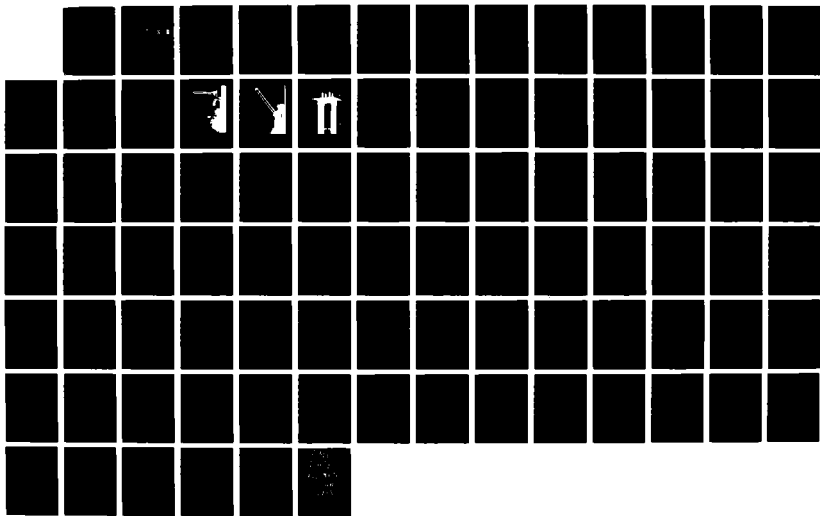
CONTROL SYSTEM SIMULATION FOR A SINGLE-LINK FLEXIBLE  
ARM(U) NAVAL POSTGRADUATE SCHOOL MONTEREY CA K S PARK  
SEP 87

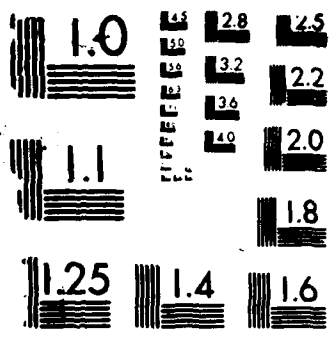
1/1

UNCLASSIFIED

F/G 13/7

NL





MICROCOPY RESOLUTION TEST CHART  
NATIONAL BUREAU OF STANDARDS 1963-A

AD-A187 037

DTIC FILE COPY

2

# NAVAL POSTGRADUATE SCHOOL

Monterey, California



DTIC  
ELECTE  
DEC 14 1987  
S D

## THESIS

CONTROL SYSTEM SIMULATION  
FOR A SINGLE-LINK FLEXIBLE ARM

by

Ki Soon Park

September 1987

Thesis Advisor

Liang-Wey Chang

Approved for public release; distribution is unlimited

87 12 3 10

REPORT DOCUMENTATION PAGE

1a REPORT SECURITY CLASSIFICATION UNCLASSIFIED		1b RESTRICTIVE MARKINGS	
2a SECURITY CLASSIFICATION AUTHORITY		3 DISTRIBUTION/AVAILABILITY OF REPORT Approved for public release; distribution is unlimited.	
2b DECLASSIFICATION/DOWNGRADING SCHEDULE		5 MONITORING ORGANIZATION REPORT NUMBER(S)	
3 PERFORMING ORGANIZATION REPORT NUMBER(S)		7a NAME OF MONITORING ORGANIZATION Naval Postgraduate School	
6a NAME OF PERFORMING ORGANIZATION Naval Postgraduate School	6b OFFICE SYMBOL (if applicable) 69	7b ADDRESS (City, State and ZIP Code) Monterey, California 93943-5000	
6c ADDRESS (City, State and ZIP Code) Monterey, California 93943-5000		9 PROCUREMENT INSTRUMENT IDENTIFICATION NUMBER	
8a NAME OF FUNDING SPONSORING ORGANIZATION	8b OFFICE SYMBOL (if applicable)	10 SOURCE OF FUNDING NUMBERS	
8c ADDRESS (City, State and ZIP Code)		PROGRAM ELEMENT NO	PROJECT NO
		TASK NO	WORK UNIT ACCESSION NO
11 TITLE (include Security Classification) CONTROL SYSTEM SIMULATION FOR A SINGLE LINK FLEXIBLE ARM			
12 PERSONAL AUTHOR(S) Park, ki Soon			
13a TYPE OF REPORT Master's Thesis	13b TIME COVERED FROM _____ TO _____	14 DATE OF REPORT (Year Month Day) 87 sept.	15 PAGE COUNT 88
16 SUPPLEMENTARY NOTATION			
17 COSAT CODES		18 SUBJECT TERMS (Continue on reverse if necessary and identify by block number)	
FIELD	GROUP	SUB-GROUP	
		Flexible Manipulator.	
19 ABSTRACT (Continue on reverse if necessary and identify by block number) To control a lightweight manipulator, a validated dynamic model based on the Equivalent Rigid Link System (ERLS), is used to formulate a control algorithm. The required torque to drive the manipulator to a desired angle is calculated. Since the control system includes an electrohydraulic actuator, the required current is also calculated by the inverse dynamics of the hydraulic servo. A computer simulation is performed with various loading conditions, gain values, and desired angles.			
20 DISTRIBUTION AVAILABILITY OF ABSTRACT <input type="checkbox"/> UNCLASSIFIED/UNLIMITED <input type="checkbox"/> SAME AS RPT <input type="checkbox"/> DTIC USERS		21 ABSTRACT SECURITY CLASSIFICATION UNCLASSIFIED	
22a NAME OF RESPONSIBLE INDIVIDUAL Prof. Chang, Code 69CK		22b TELEPHONE (include Area Code) 2532	22c OFFICE SYMBOL 69CK

Approved for public release; distribution is unlimited.

Control System Simulation  
for a Single-Link Flexible Arm

by

Ki Soon Park  
Major, Republic of Korean Air Force  
B.S., Korean Air Force Academy 1978  
M.B.A., Chungnam University of Korea 1984

Submitted in partial fulfillment of the  
requirements for the degree of

MASTER OF SCIENCE IN MECHANICAL ENGINEERING

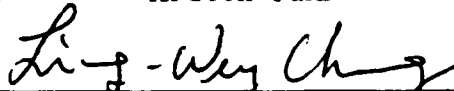
from the

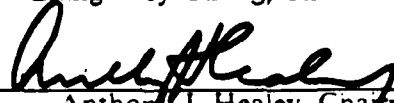
NAVAL POSTGRADUATE SCHOOL  
September 1987

Author:

  
Ki Soon Park

Approved by:

  
Liang-Wey Chang, Thesis Advisor

  
Anthony J. Healey, Chairman,  
Department of Mechanical Engineering

  
Gordon E. Schacher,  
Dean of Science and Engineering

## ABSTRACT

To control a lightweight manipulator, a validated dynamic model based on the Equivalent Rigid Link System (ERLS), is used to formulate a control algorithm. The required torque to drive the manipulator to a desired angle is calculated. Since the control system includes an electrohydraulic actuator, the required current is also calculated by the inverse dynamics of the hydraulic servo. A computer simulation is performed with various loading conditions, gain values, and desired angles.



Accession For	
NTIS CRA&I	<input checked="" type="checkbox"/>
DTIC TAB	<input type="checkbox"/>
Unannounced	<input type="checkbox"/>
Justification	
By	
Distribution/	
Availability Codes	
Dist	Avail and/or Special
A-1	

## TABLE OF CONTENTS

I.	INTRODUCTION .....	10
	A. MOTIVATION .....	10
	B. NATURE OF THE PROBLEM .....	10
	C. LITERATURE REVIEW .....	11
	D. RESEARCH OBJECTIVE .....	12
II.	MODEL FORMULATION FOR A SINGLE LINK FLEXIBLE MANIPULATOR .....	13
	A. PHYSICAL PLANT .....	13
	B. EQUIVALENT RIGID LINK SYSTEM FOR A SINGLE- LINK MANIPULATOR .....	13
	C. SHAPE FUNCTION DERIVATION .....	20
	D. HYDRAULIC ACTUATION .....	21
III.	CONTROL SCHEME .....	24
	A. REQUIRED TORQUE .....	24
	B. REQUIRED CURRENT .....	26
IV.	RESULT .....	29
	A. INPUTS AND MOTION OUTPUTS .....	29
	B. REQUIRED TORQUES .....	31
	C. CURRENT CALCULATIONS .....	32
	D. THE REDUCTIONS OF THE REQUIRED TORQUE .....	33
	E. THE REDUCTION OF VIBRATION .....	34
	F. THE ELECTROHYDRAULIC SATURATION .....	35
V.	CONCLUSIONS AND RECOMMENDATIONS .....	62
	A. CONCLUSIONS .....	62
	B. RECOMMENDATIONS .....	63

APPENDIX A: DERIVATION OF THE EQUATIONS OF MOTION FOR THE SINGLE - LINK FLEXIBLE MANIPULATOR .....	64
APPENDIX B: SIMULATION PROGRAM .....	71
LIST OF REFERENCES .....	85
INITIAL DISTRIBUTION LIST .....	86

## LIST OF TABLES

1. ARM PARAMETERS .....	14
2. INITIAL CONDITIONS .....	29
3. GAIN VALUES .....	30
4. MAXIMUM OF TOTAL-ANGLE VELOCITY AND TOTAL-ANGLE ACCELERATION .....	32
5. MAXIMUM REQUIRED TORQUE .....	33
6. MAXIMUM TORQUE FOR INPUT FUNCTIONS .....	34

## LIST OF FIGURES

2.1	A Single-Link Flexible Manipulator System	15
2.2	A Manipulator in Intermediate Position with 2.115kg Loading	15
2.3	Details of Transverse Bridges and Tip Loading	16
2.4	The Equivalent Rigid Link System (ERLS)	17
2.5	An overall Plant	22
3.1	A Schematic Diagram of the Feedback Control System	27
4.1	Total Angle Response ( 0 kg )	36
4.2	Total Angle Response ( 2.115 kg )	36
4.3	Total Angle Response ( 4.233 kg )	37
4.4	Total-Angle Velocity (4.233kg)	38
4.5	Total-Angle Acceleration(4.233kg)	39
4.6	Total Angle Responses for Various Desired Angles(2.115kg)	40
4.7	Total-Angle Velocities for Various Desired Angles(2.115kg)	41
4.8	Total-Angle Accelerations for Various Desired Angles(2.115kg)	43
4.9	Required Torque ( 0 kg )	43
4.10	Required Torque ( 2.115 kg )	44
4.11	Required Torque ( 4.233 kg )	45
4.12	Required Torques for Various Desired Angles(2.115kg)	46
4.13	Required Current (0 kg )	47
4.14	Required Current (2.115 kg )	48
4.15	Required Current (4.233 kg )	49
4.16	A Planned Input of the Desired Angle(4.233 kg )	50
4.17	Total Angle Responses for Various Input Functions(4.233kg)	51
4.18	Required Torques for Various Input Functions(4.233 kg )	52
4.19	Require Currents for Various Input Functions(4.233kg)	53
4.20	Total Angle Responses for Various Damping Ratios(no load )	54
4.21	Large motion for Various Damping Ratios (no load )	55
4.22	Small Motion for Various Damping Ratios (no load )	56

4.23	Required Torque for Various Damping Ratios (no load )	57
4.24	Required Currents for the Ideal and Saturated cases(4.233kg)	58
4.25	Required Torques for the Ideal and Saturated cases(4.233 kg )	59
4.26	Total Angle Responses for the Ideal and Saturated cases(4.233kg)	60

## ACKNOWLEDGEMENT

I wish to express my sincerest gratitude to my advisor, Professor Liang-Wey Chang, for his invaluable guidance and unselfish giving of his time in support of this research.

Appreciation is extended to the Korean Air Force Authority for the opportunity to study in Naval Postgraduate School.

I also want to thank my wife, Mi Sook and my daughter, Soo Yeun for their patience and encouragement in my study.

## I. INTRODUCTION

### A. MOTIVATION

The robotic manipulator plays an important role in a wide range of applications. Present and possible future applications focus on implementing automation in environments which are hostile to humankind. More demand is being placed on robots with higher speeds, smaller actuators, and higher payload capacity in applications.

In the past, efforts were made to control manipulators using rigid body assumptions. However, the demands for lightweight and higher performance manipulators have led to the consideration of flexible-body models. A new controller is needed for the flexible manipulators.

### B. NATURE OF THE PROBLEM

Control of most manipulators is based upon dynamic models assuming perfectly rigid links. Accordingly, accurate manipulator motion control is dependent upon the great stiffness of the structural members. This assumption does not always hold, particularly at high-speed and heavy-load operations where a linkage may undergo severe elastic deformation due to the inertia. It can no longer perform its intended function in actual operations.

Lightweight flexible manipulators promise the advantages of increased speed of operation, ease of transportability, reduced material requirement, reduced power consumption, lowered mounting strength and rigidity requirement, and lower overall cost [Ref. 1]. On the other hand, the oscillatory behavior of the flexible links makes the end-point motions difficult to be controlled. The central problem lies in the control of the end-point motion by applying the proper torques at the actuating point. Flexibility effect on manipulators is a necessary consideration in the move toward designing lighter, faster and more accurate robot systems. A dynamics model of manipulators with flexibility is needed for design and control purposes. To benefit from the advantages of lightweight, flexible manipulators, it is also necessary to implement a control design capable of achieving end effector positioning accuracy and stable control.

### C. LITERATURE REVIEW

The earliest studies concerning the control of flexible manipulators began in the early to mid 1970's. There has been considerable research recently in the development of flexible manipulator control strategies. A brief survey of this research follows.

Book [Ref. 2] introduced a modeling approach utilizing  $4 \times 4$  transformation for control purposes. His model was limited in the assumption that the mass of the manipulator is negligible compared to the mass of the load. The assumption is acceptable in space applications where the manipulator is very light and operates at low speeds, but the assumption can not be applied to the industrial robotic manipulators in most cases.

Sunada and Dubowsky [Ref. 3] applied  $4 \times 4$  transformation matrix and the Lagrangian approach to model the flexible system with geometrically irregular links by finite element techniques. Component Mode Synthesis was used to reduce the number of generalized coordinates and improve the computational efficiency without losing much accuracy. Based on this scheme, they can obtain the flexibility and mass properties of the links through available finite element programs. But, this model ignored the effect of the small motion interaction on the large motion. The consideration of the coupling effect between the small motion and the large motion was not completed.

Chang [Ref. 4] introduced the Equivalent Rigid Link System(ERLS) dynamic model of flexible manipulator. Global motions were separated into large motions and small motions. The ERLS described the kinematics of the large motion. The small motion displacements were described relative to the ERLS. The finite element method was used to discretize deformations and Lagrangian formation was used to derive the equations of motion. Two sets of coupled, non-linear ordinary differential equations - large motion equations and small motion equations resulted. The set of large motion equations were non-linear in both the large and small motion variables. The set of small motion equations were linear in the small motion variable but non-linear in the large motion variable. The model is complete being able to describe large motions, small motions and their coupling. The model presented the computational potential by using the Sequential Integration Method developed.

Petroka [Ref. 5] performed an experimental validation of the ERLS model. He designed a hydraulically actuated, single - link flexible arm. A cubic shape function was assumed to present the transverse displacement of the flexible manipulator. Tip position was determined from the motion picture studies.

Gannon [Ref. 6] served a continuation of the experimental validation of the ERLS model. A piezo-resistive accelerometer and strain gages were used for tip position and strain information. The natural mode shape functions of a beam was used to present the flexural motion of the single-link flexible arm in the Gannon's study. Results of the validation suggested the potential usefulness of the model in determining tip position.

Canon and Schmitz [Ref. 7] reported on experimental studies of the "End - Point Control of a Flexible One Link Robot". Their controller design was based upon a linearized and truncated model. Measurements available for control included rigid body angle and velocity, strain measurements and direct optical measurement of end-point position. Controller design was discussed from a variety of standpoints using both classical and modern control methods. The authors reported that the non-colocated(end -point position) feedback improves the speed of response at the cost of reducing the stability margins.

Flexibility effect is a very important consideration in designing lighter, faster and more accurate robot systems. In this research, the ERLS dynamic model is used to design a control system since the model presents a complete consideration of the system motion and exhibits computational superiority. Nonlinear motion is compensated in the control algorithm.

#### **D. RESEARCH OBJECTIVE**

The objective of this research is to design a controller for single-link flexible manipulator. The validated dynamic model-the Equivalent Rigid Link System - is used to formulate the control algorithm. The control algorithm involves the computation of the required torque to drive the manipulator achieving a desired angle of the end of the flexible manipulator. Since the control system includes an electrohydraulic actuator, the required current is also calculated by inverse hydraulic dynamics. The ways to reduce the actuator effort and structural vibrations will be discussed.

## II. MODEL FORMULATION FOR A SINGLE LINK FLEXIBLE MANIPULATOR

### A. PHYSICAL PLANT

A flexible arm was designed by Petroka [Ref. 5] for the validation of the Equivalent Rigid Link System Model. The flexible arm shown in Figures 2.1 - 2.2 is a one meter long flexible structure which can be bend freely in the vertical plane but is stiff in the torsion and horizontal bending. The basic configuration of the arm includes two parallel, flexible steel, flat bars connected by the thin steel strips to transverse steel bridges. External loading is attached to the arm tip end transverse bridge by the securing of the load on the four welded studs shown in Figure 2.3. Table 1 shows the geometric and mass properties of the flexible arm. The flexible arm is driven by a electrohydraulic system shown in Figure 2.1. The system consists of a York hydraulic power unit, a Berd- Johnson 3 - axis Hyd-Ro- Wrist, a Moog 760-100 servovalve, and associated Moog servocontroller and high pressure filter assembly [Ref. 5].

### B. EQUIVALENT RIGID LINK SYSTEM FOR A SINGLE-LINK MANIPULATOR

The basic idea of ERLS [Ref. 4] is to separate the motion of the flexible link system into the large rigid-body motion and the small-motion displacement due to the flexibility of the structure. The large motion is defined by the movement of ERLS for a single - link flexible manipulator. The small-motion displacements are described with respect the ERLS. A schematic diagram of the ERLS for a single - link manipulator is shown in Figure 2.4.

The three generalized coordinates chosen are the large motion joint variable,  $\theta$ , and two nodal displacements,  $V(0)$  and  $\varphi(0)$ , which can be measured at the end of the link. The large motion joint variable,  $\theta$ , is the angle between the ERLS and the horizontal axis of inertia coordinate. Homogenous transformations is applied for a deformed point on the single-link to obtain the absolute position of the point. The displacements for each point along the flexible arm are the functions of the location and time; therefore, it is necessary to discretize the deformations in terms of generalized coordinates in order to apply Lagrangian's equation. The techniques of the Finite Element Method (FEM) are utilized for this discretization. The nodal displacements at the end of the single-link represent the small motion.

TABLE 1  
ARM PARAMETERS

Parameter	Value	Unit
Arm Length (L)	0.9985	m
Beam Thickness(t)	0.003175	m
Beam Width(w)	0.0762	m
Distance Between Each Beam	0.05715	m
Arm Mass( $m_t$ )	4.8565	kg
Modulus of Elasticity(E)	2.0 E11	N/m <sup>2</sup>
Density/unit Volume( $\rho$ )	7861.05	kg/m <sup>3</sup>

After describing the kinematics relationships between the large and small motions, kinetics is introduced to complete the derivation of the equation motion.

The Lagrangian dynamics approach is used for the derivation due to its straightforward and systematic nature which is helpful in the analysis of complex systems. The kinetic energy is the sum of the kinetic energies of each link, actuator, and any loading. The potential energy is contributed the elastic strain energy and from gravity. Generalized forces are included due to any applied forces and damping forces. After making considerable effort in mathematical manipulations, rearrangements, and simplifications, the Lagrangian equations yield two sets of non-linear, coupled, second-order, ordinary differential equations. One set describes the large motions and the other set describes the small motions.

These equations are represented as follow;

$$M_{qq} \ddot{\theta} + M_{qn} \ddot{U} = F_q + \text{TORQUE} \quad (2.1)$$

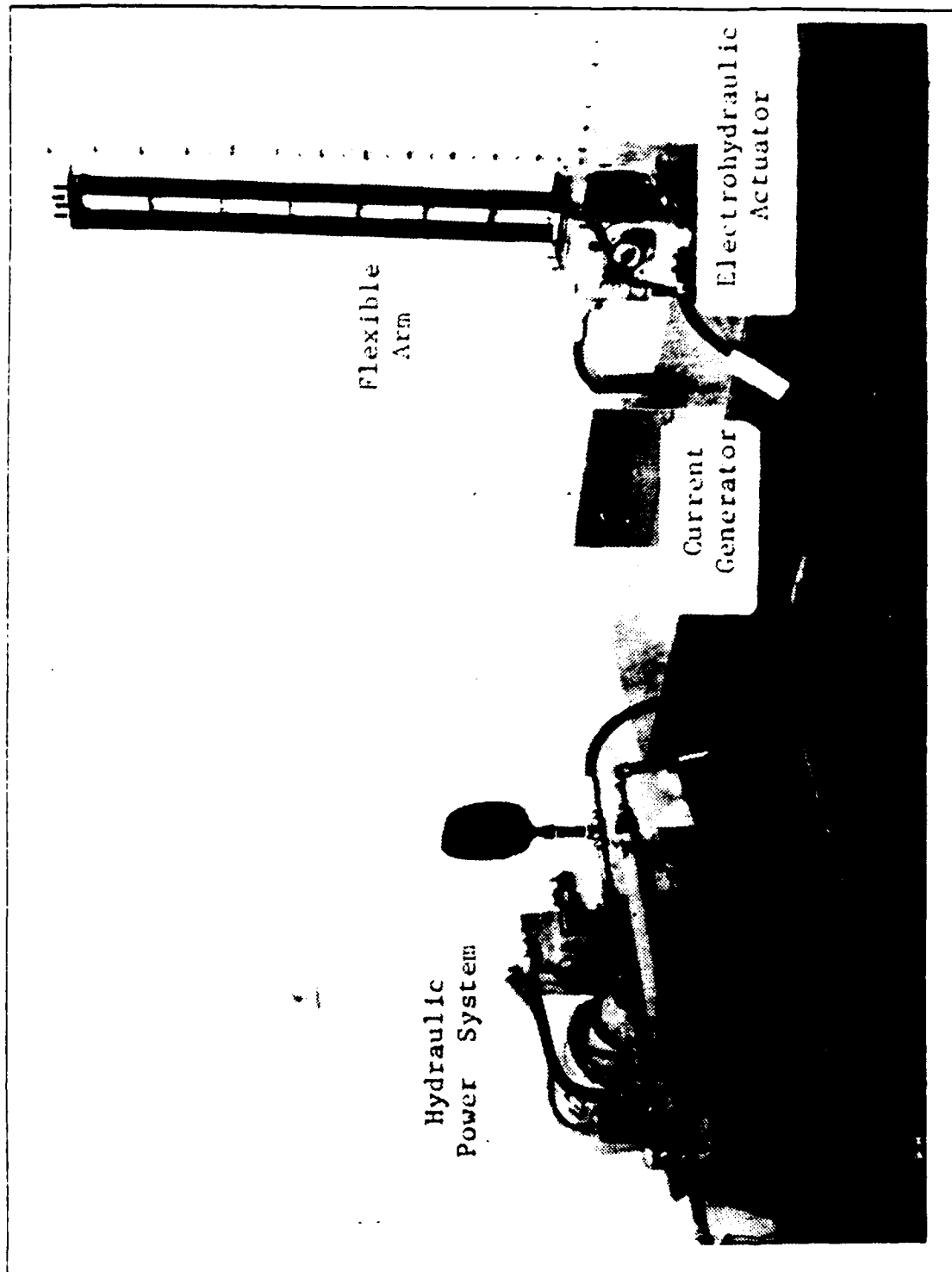


Figure 2.1 A Single-Link Flexible Manipulator System.

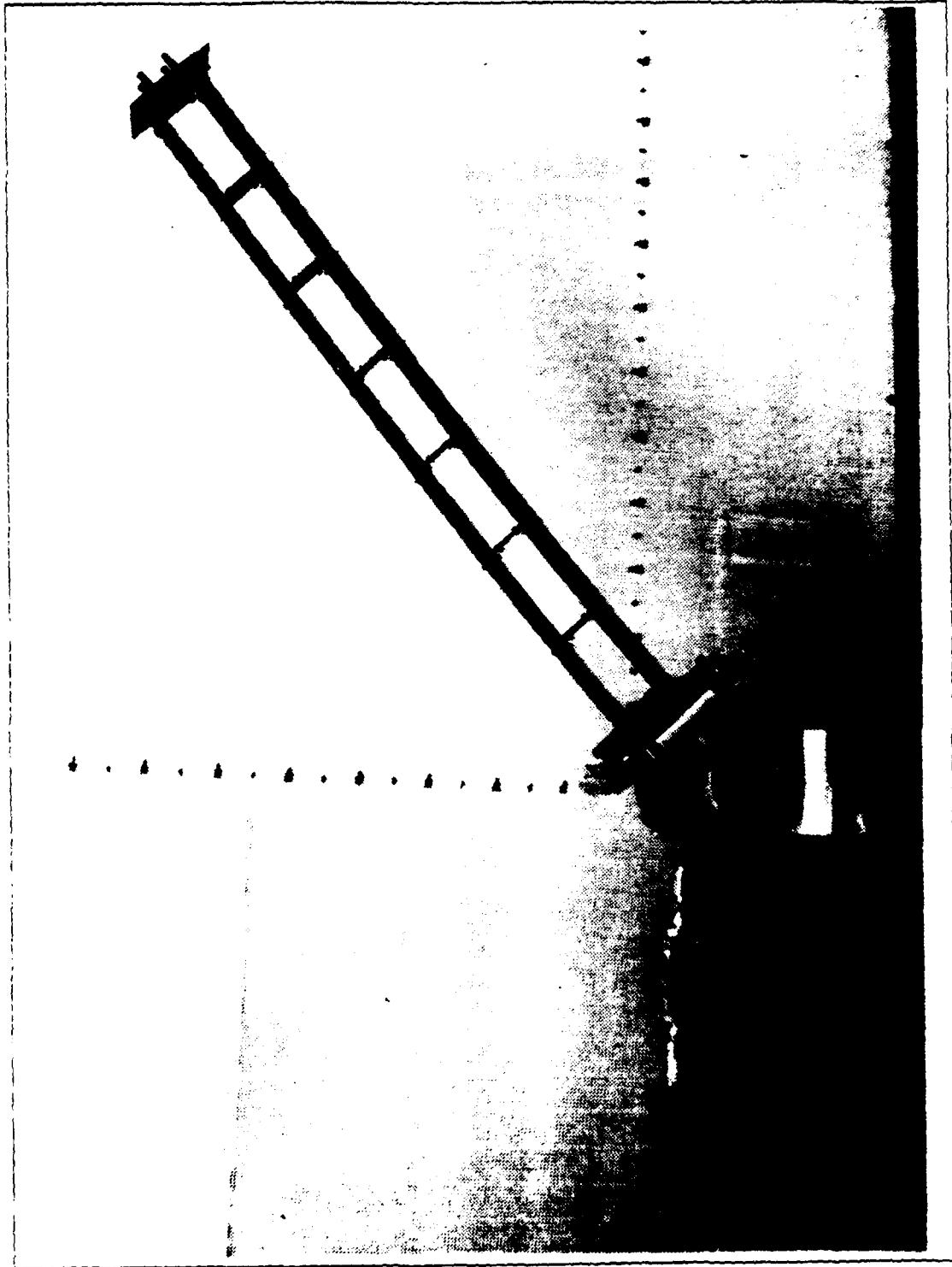


Figure 2.2 A Manipulator in Intermediate Position with 2.115kg Loading.

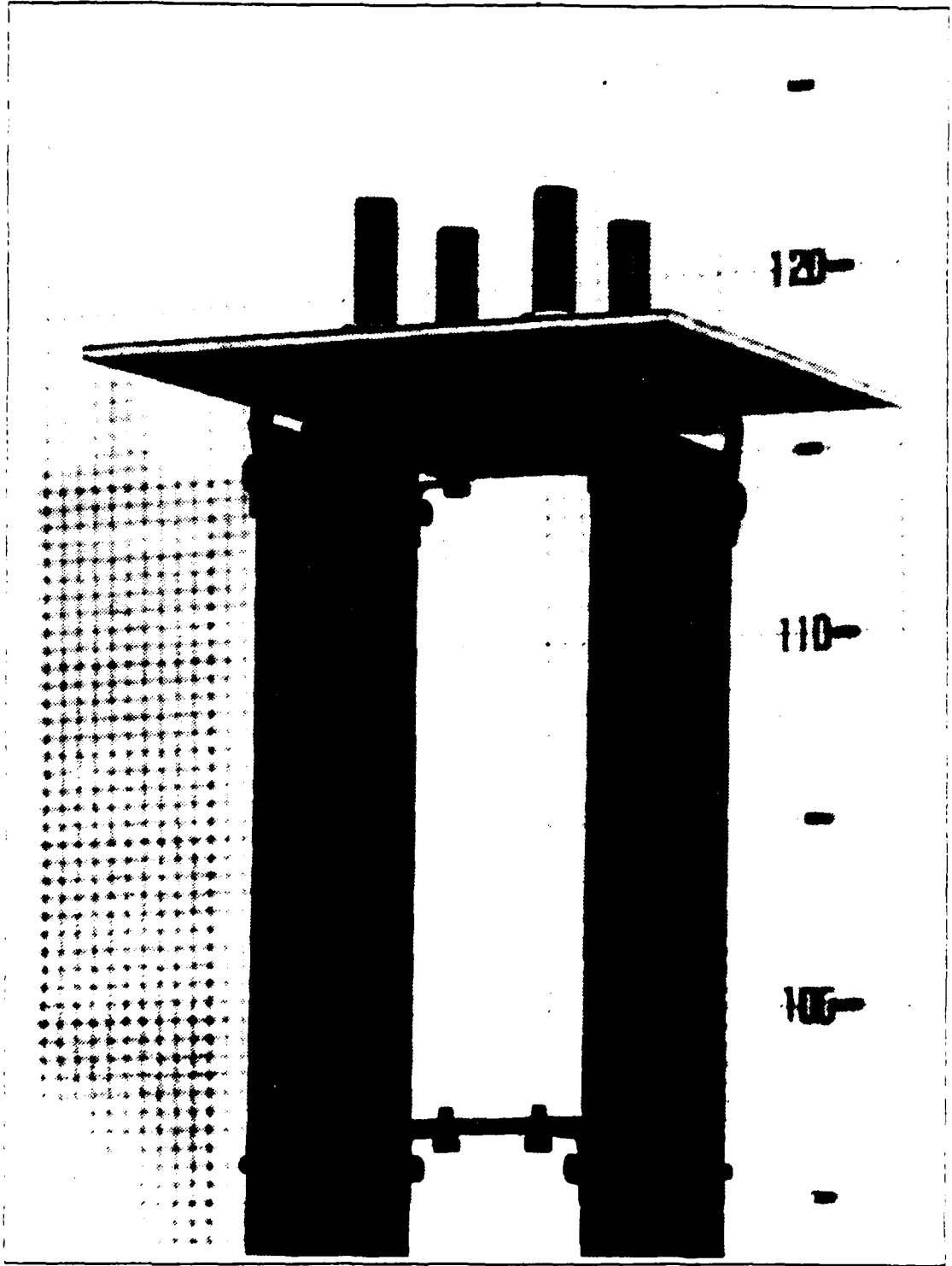


Figure 2.3 Details of Transverse Bridges and Tip Loading.

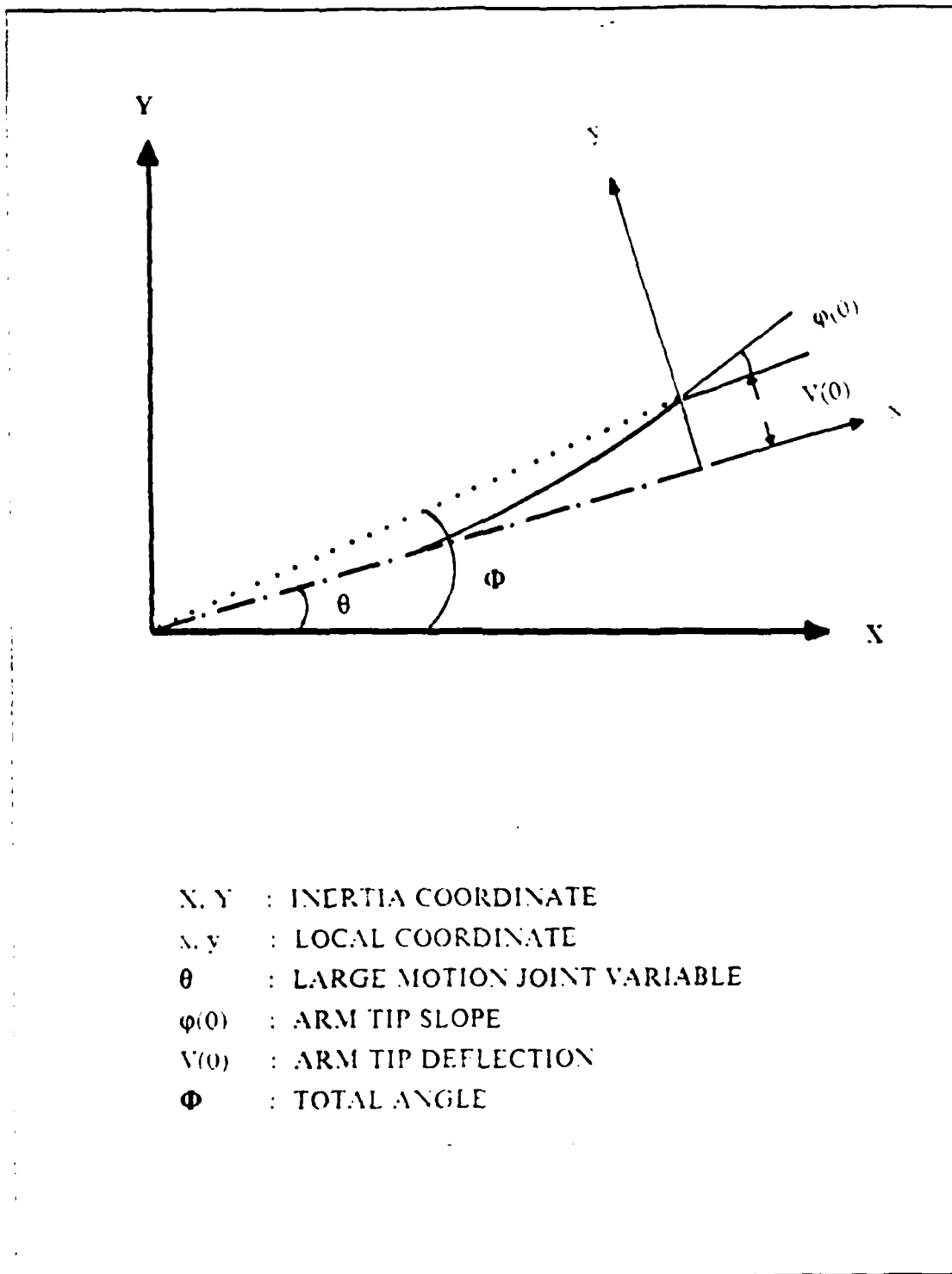


Figure 2.4 The Equivalent Rigid Link System (ERLS).

$$M_{nq} \ddot{\theta} + M_{nn} \ddot{U} + K_n U = F_n \quad (2.2)$$

where

- $M_{qq}$  = 1 × 1 effective inertia matrix for large motions
- $M_{qn}$  = 1 × 2 coupled inertia matrix of the small motion effect on large motions
- $M_{nq}$  = 2 × 1 coupled inertia matrix of the large motion effect on the small motions
- $M_{nn}$  = 2 × 2 effective inertia matrix for small motions
- $K_n$  = 2 × 2 stiffness matrix for small motions
- $F_q$  = 1 × 1 load vector for large motions
- $F_n$  = 2 × 1 load vector for small motions
- $\theta$  = generalized coordinate of the large motions
- $U$  = 2 × 1 generalized coordinate of the small motions

The vector of small motion is limited to the transverse displacement of the end of the link. Axial deformation and torsion are neglected in this research for single-link manipulators. We assume that the displacement of the end of the link is small.

$$\text{Tan}^{-1}(V/L) \sim V/L \quad (2.3)$$

where  $V$  is a shorthand of  $V(0)$ .

We also assume that the slope of the arm tip is not measured for the simple feedback control system. The tip displacement  $V(0)$  is the only generalized coordinate chosen for small motions. Then all coefficient of the matrixs of non-linear, coupled, second-order ordinary differential equations is reduced to 1 × 1 matrix. A total angle of the end of the link can be represented as follows;

$$\Phi = \theta + V/L \quad (2.4)$$

$$\dot{\Phi} = \dot{\theta} + \dot{V}/L \quad (2.5)$$

$$\ddot{\Phi} = \ddot{\theta} + \ddot{V}/L \quad (2.6)$$

A more detailed derivation of the equations of motion is included in Appendix A.

### C. SHAPE FUNCTION DERIVATION

The natural-mode shape function of a beam is needed to present the flexural motion of the single-link flexible arm [Ref. 4]. The flexible manipulator arm is modeled as a continuous Euler-Bernoulli cantilever beam. The transverse displacement for the single link flexible arm is represented in the following forms;

$$\begin{aligned} U(x,t) &= a_1(t) \chi_1(x) + a_2(t) \chi_2(x) \\ &= a_1 \{ A_1' \{ \cos\beta_1 x + \cosh\beta_1 x \} + \{ \sin\beta_1 x + \sinh\beta_1 x \} \} \\ &\quad + a_2 \{ A_2' \{ \cos\beta_2 x + \cosh\beta_2 x \} + \{ \sin\beta_2 x + \sinh\beta_2 x \} \} \end{aligned} \quad (2.7)$$

where

$$\beta_1 L = 1.875104069$$

$$\beta_2 L = 4.694091133$$

$$A_i' = \frac{\sin\beta_i L + \sinh\beta_i L}{\cos\beta_i L + \cosh\beta_i L} \quad (2.8)$$

Upon reduction, Gannon [Ref. 6] yielded a  $3 \times 2$  shape function matrix  $\Psi$ , and the  $2 \times 1$  nodal displacement vector,  $U$ . a  $3 \times 1$  deformation vector,  $d$ , was expressed as follow;

$$d = \Psi U = \begin{bmatrix} 0 \\ 0 \\ V(x) \end{bmatrix} = \begin{bmatrix} 0 & 0 \\ 0 & 0 \\ M & N \end{bmatrix} \begin{bmatrix} V(0) \\ \phi(0) \end{bmatrix}$$

The coefficients  $M$  and  $N$  are defined as;

$$\begin{aligned} M &= \{ C_1 \{ A_1' \{ \cos\beta_1 x + \cosh\beta_1 x \} + \{ \sin\beta_1 x + \sinh\beta_1 x \} \} \\ &\quad + C_2 \{ A_2' \{ \cos\beta_2 x + \cosh\beta_2 x \} + \{ \sin\beta_2 x + \sinh\beta_2 x \} \} \} \\ N &= \{ C_3 \{ A_1' \{ \cos\beta_1 x + \cosh\beta_1 x \} + \{ \sin\beta_1 x + \sinh\beta_1 x \} \} \} \end{aligned}$$

$$+ C_4 \{ A_2' \{ \cos \beta_2 x + \cosh \beta_2 x \} + \{ \sin \beta_2 x + \sinh \beta_2 x \} \}$$

where

$$C_1 = 2 \beta_2' / \{ 4 A_1' \beta_2 - 4 A_2' \beta_1 \}$$

$$C_2 = -2 \beta_1' / \{ 4 A_1' \beta_2 - 4 A_2' \beta_1 \}$$

$$C_3 = -2 A_2' / \{ 4 A_1' \beta_2 - 4 A_2' \beta_1 \}$$

$$C_4 = 2 A_1' / \{ 4 A_1' \beta_2 - 4 A_2' \beta_1 \}$$

In this research, since the slope function of the arm tip is not measured, the shape function,  $\Psi$ , is reduced to a  $3 \times 1$  matrix. Now the  $3 \times 1$  deformation vector can be rewritten as follows;

$$d = \Psi U = \begin{bmatrix} 0 \\ 0 \\ V(x) \end{bmatrix} = \begin{bmatrix} 0 \\ 0 \\ M \end{bmatrix} \begin{bmatrix} V(0) \end{bmatrix}$$

New shape function matrix is now in a convenient form for computer coding. A more detailed derivation of the shape function was included in Gannon's work.

#### D. HYDRAULIC ACTUATION

The single-link flexible manipulator uses electrohydraulic actuation to drive the plant. The inclusion of the electrohydraulic power system involves the transformation of an input current to an output torque. Figure 2.5 illustrates the relationship of hydraulic dynamics to the overall system.

The hydraulic dynamics is represented by servovalve dynamics and actuator dynamics. Moog, the manufacture of the servovalve, simplified the description of servovalve dynamics to a single equation [Ref. 8].

$$Q = I K \sqrt{P_v} \quad (2.9)$$

where

Q = flow delivered from servovalve

I = input current

K = valve sizing constant, contributes to hydraulic system damping

$P_v$  = valve pressure drop,  $P_s - P_L$

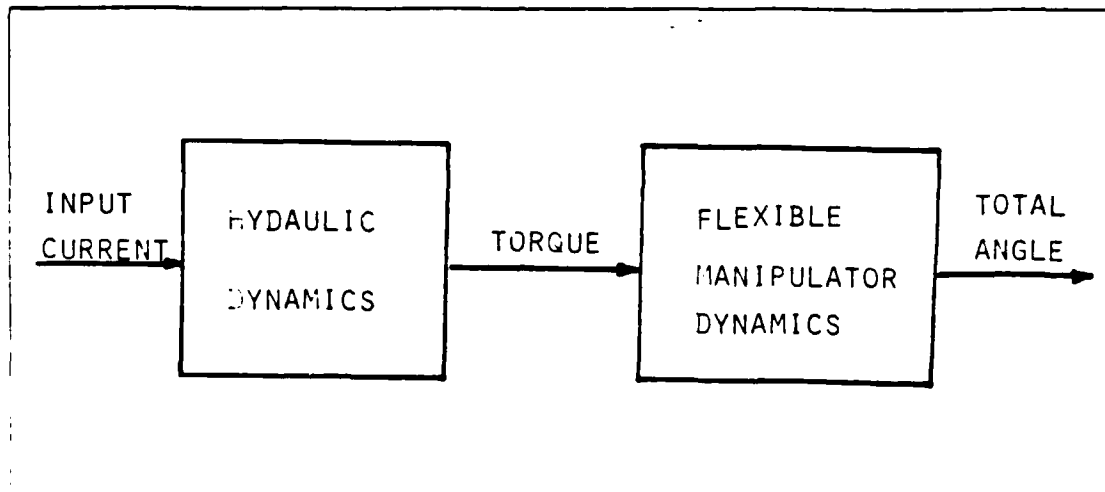


Figure 2.5 An overall Plant.

Actuator dynamics consists of a form of the continuity equation and the torque output equation. Actuator dynamics consists of a form of the continuity equation and the torque output equation [Ref. 9].

$$Q = D_m \dot{\theta} + C_{tm} P_L + \frac{V_t \dot{P}_L}{4 \beta_e} \quad (2.10)$$

$$T_d = \eta_t P_L D_{td} \quad (2.11)$$

Where

$Q$  = flow delivered to actuator

$D_m \dot{\theta}$  = flow causing actuator rotation

$\beta_e$  = effective bulk modulus of fluid

$V_t$  = total compressed volume including actuator lines and chambers

$V_t \dot{P}_L / (4 \beta_e)$  = compressibility flow

$T_d$  = torque required to overcome inertia and move the load

$\eta_t$  = torque efficiency

$P_L$  = load pressure drop

$D_m$  = motor displacement

$C_{tm} P_L$  = leaking flow in actuator

The preceding hydraulic dynamic equations and relationships are incorporated into the main computer program for solving the dynamic equation of motion.

### III. CONTROL SCHEME

#### A. REQUIRED TORQUE

In feedback control system, desired angles are compared with the measurements of the actual system responses. The difference is used via the chosen control algorithm. The control algorithm calculates the required torque to derive the manipulator achieving a desired angle of the end of the arm.

Recall the equations that can be written as two sets of equations - large motions and small motions equations - and the total angle equation of the end of the arm for derivation of the required torque equation.

$$M_{qq} \ddot{\theta} + M_{qn} \ddot{v} = F_q + \text{TORQUE} \quad (3.1)$$

$$M_{nq} \ddot{\theta} + M_{nn} \ddot{v} + K_n v = F_n \quad (3.2)$$

where

- $M_{qq}$  = 1 × 1 effective inertia matrix for large motions
- $M_{qn}$  = 1 × 1 coupled inertia matrix of the small motion effect on large motions
- $M_{nq}$  = 1 × 1 coupled inertia matrix of the large motion effect on the small motions
- $M_{nn}$  = 1 × 1 effective inertia matrix for small motions
- $K_n$  = 1 × 1 stiffness matrix for small motions
- $F_q$  = 1 × 1 load vector for large motions
- $F_n$  = 1 × 1 load vector for small motions
- $\theta$  = generalized coordinate of the large motions
- $v$  = 1 × 1 generalized coordinate of the displacements

$$\theta = \Phi - v L \quad (3.3)$$

$$\dot{\theta} = \dot{\Phi} - \dot{V}/L \quad (3.4)$$

$$\ddot{\theta} = \ddot{\Phi} - \ddot{V}/L \quad (3.5)$$

Equations 3.3-3.5 can be substituted into Equations 3.1 and 3.2 and rearranged as follows;

$$M_{qq} (\ddot{\Phi} - \ddot{V}/L) + M_{qn} \ddot{V} - F_q = \text{TORQUE} \quad (3.6)$$

$$M_{nq} (\ddot{\Phi} - \ddot{V}/L) + M_{nn} \ddot{V} + K_n V - F_n = 0 \quad (3.7)$$

After eliminating  $V$ , a governing equation for  $\Phi$  is given as;

$$(M_{qq} - D M_{nq}) \ddot{\Phi} + (D F_n - D K_n - F_q) V = \text{TORQUE} \quad (3.8)$$

where

$$D = \frac{(M_{qn} - (M_{qq}/L))}{(M_{nn} - (M_{nq}/L))} \quad (3.9)$$

Let

$$N = M_{qq} - D M_{nq}$$

Equation 3.8 can be expressed in short as follows;

$$N \ddot{\Phi} + FC(V, \dot{V}, \theta, \dot{\theta}) = \text{TORQUE} \quad (3.10)$$

where

$$FC(V, \dot{V}, \theta, \dot{\theta}) = (D F_n - D K_n - F_q) V$$

$\Phi$  is measured and fed back to controller. The required torque to drive the manipulator achieving a desired angle of the end of the arm is calculated via a controller. The inverse problem is applied to calculate the required torque. Figure 3-1 shows a schematic diagram of the feedback control system.

The equation of the required torque is represented as follows;

$$T_r = N (\ddot{\Phi}_d + K_v (\dot{\Phi}_d - \dot{\Phi}) + K_p (\Phi_d - \Phi)) + FC \quad (3.11)$$

where

- $T_r$  = a required torque
- $\ddot{\Phi}_d$  = a desired angular acceleration
- $\ddot{\Phi}$  = a total angular acceleration
- $\dot{\Phi}_d$  = a desired angular velocity
- $\dot{\Phi}$  = a total angular velocity
- $\Phi_d$  = a desired angle
- $\Phi$  = a total angle
- $K_v$  = a velocity gain
- $K_p$  = a position gain

The torque of the Equation 3.10 is equals to the required torque of the Equation 3.11. System errors of a second order control system can be represented as follows;

$$(\ddot{\Phi}_d - \ddot{\Phi}) + K_v (\dot{\Phi}_d - \dot{\Phi}) + K_p (\Phi_d - \Phi) = 0 \quad (3.12)$$

## B. REQUIRED CURRENT

Since the control system includes an electrohydraulic actuator, the inverse hydraulic dynamic involves the transformation of input torque to an output current. For the input current to the hydraulic dynamics, the inverse hydraulic dynamics can be applied to calculate the required current according to the required torque. A desired load pressure drop and desired flow should be calculated by the inverse hydraulic dynamic equations.

$$P_{Lr} = T_d / (\eta_t D_m) \quad (3.13)$$

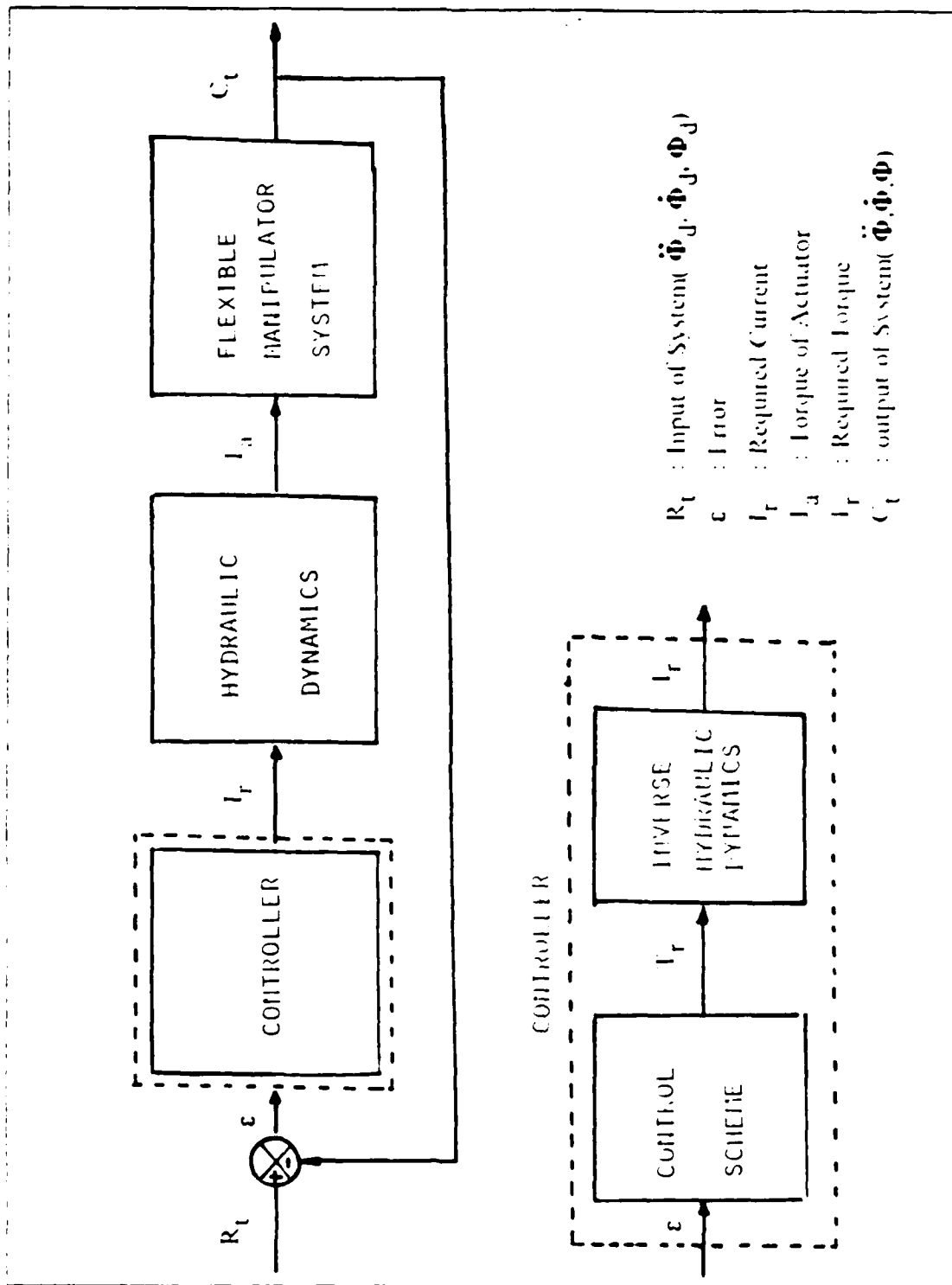


Figure 3.1 A Schematic Diagram of the Feedback Control System.

$$Q_r = D_m \dot{\theta} + C_{tm} P_{Lr} + (V_t \dot{P}_{Lr}) / (4 B_e) \quad (3.14)$$

$$I_r = Q_d / (K \sqrt{P_v}) \quad (3.15)$$

where

$T_r$  = a required torque

$P_{Lr}$  = a required load pressure drop

$Q_r$  = a required flow delivered to actuator

$I_r$  = a required current

## IV. RESULT

A control algorithm for a single-link flexible manipulator is based upon the Equivalent Rigid Link System Model. The control algorithm calculates the required torque to control the end position of the manipulator. Comparisons of the required torque and required current are made in terms of the three parameters (i.e., loading condition, gain value, and desired angle). Additionally, the way to reduce the required currents and required torques is discussed. The effect of the current saturation to system dynamics behavior is also presented.

### A. INPUTS AND MOTION OUTPUTS

The loading conditions are no load, a 2.115 kg ,and a 4.233kg load. The external loading is attached to the arm tip end transverse bridge by securing the load on the four welded studs. The initial condition for all runs is the horizontal position of the flexible arm. The initial tip deformations as determined by the Euler-Beroulli cantilever beam theory are converted to an angle. These angles in Table 2 are the initial conditions input into the simulation program.

Load ( Kg )	Angle (radian)
0.0	-0.06111
2.115	-0.14628
4.233	-0.23155

Only point to point control in open space is considered. An input variable to the closed-loop system is the desired angle of the end-point. The desired angular acceleration and the desired angular velocity are zero in this research. To compare the

system responses, two step inputs, which are two desired angles of the end-point,(i.e., 1 radian and 1.5 radian), are applied respectively.

The outputs of the system responses for the step input of the desired angle are total-angle accelerations, total-angle velocities and total angles of the end-point, which are also fed back to the controller. First, the desired angle of 1 radian is input as the step function. Figures 4.1-4.3 show the movements of the end-point for all loading conditions. Each figure has three curves according to selected gain values for all loading conditions. In this research, a velocity gain ( $K_v$ ) and a position gain ( $K_p$ ) are selected for critically damped systems. In other words, the movements of the total angle of the end-point will not exceed the desired angle of the end-point. The position gain can be expressed in terms of the velocity gain for the critically damped systems as follows;

$$K_p = K_v^2 / 4$$

Table 3 shows the three cases of gain values for this research:

TABLE 3 GAIN VALUES		
Case	Velocity Gain	Position Gain
1	2	1
2	4	4
3	8	16

For the evaluation of the system performances for the step input, a settling time corresponding to a 2 % tolerance is measured in terms of time constant( $T = 1 / K_p^{1/2}$ ). Settling time( $t_s = 4 T$ ) are 4 sec, 2 sec and 1 sec according to the position gains 1, 4 and 16. All results of the total angles of the end-point meet error criteria of 2 % according to the gain values. The figures of the total angle of the end-point with larger gain values show faster movement. Another observation is that the total angle

of the end-point with the same gain value have the same movement in terms of the time constant for the different loading conditions. These results indicate that the nonlinear plant is controlled to perform a linear behavior. Errors of the system can be represented as the second-order control system as follows;

$$(\ddot{\Phi}_d - \ddot{\Phi}) + K_v(\dot{\Phi}_d - \dot{\Phi}) + K_p(\Phi_d - \Phi) = 0$$

Figures 4.4-4.5 show the total-angle velocity and total-angle acceleration approaching the desired angle of 1 radian for the 4.233 kg loading condition. All initial velocities start from zero and being increasing to achieve the desired angle with fast movement as gain values are increasing during transients and converge to zero velocity as the total angle of the end-point approaches to the desired angle.

Figure 4.6 shows the comparison of the total angle response for the step inputs of 1 radian and 1.5 radian with the position gain of 4, the velocity gain of 4 and 2.115 kg loading condition. The total angle movement of the 1.5 radian is faster than the movement of the desired angle of 1 radian. But both of the total angle response have same settling time since they have the same position (4) and velocity gain values(4). Figures 4.7-4.8 show the comparisons of the total-angle velocity and total-angle acceleration between the 1 radian and 1.5 radian of the desired angle with same position gain for the 2.115kg loading condition. The figures of the total-angle velocity and total-angle acceleration indicate that total-angle velocities and accelerations are increasing as desired angle is increasing with same gain value during the transients. The maximum of total-angle velocities and total-angle accelerations for the desired angles are shown in Table 4.

## B. REQUIRED TORQUES

In the feedback control system, the desired angle of the end-point is compared with the measurements of the actual system responses. The differences are used via the chosen control algorithm to calculate the required torque. In other words, the control algorithm calculates the required torques to drive the manipulator to achieve the desired angle of the end-point according to the chosen gain values. The equation of the required torque was represented as follows;

$$T_r = N(\ddot{\Phi}_d + K_v(\dot{\Phi}_d - \dot{\Phi}) + K_p(\Phi_d - \Phi)) + FC$$

TABLE 5  
MAXIMUM REQUIRED TORQUE

Load(kg)	Postion Gain	Torque(N-m)
No Load	1	82.559
	4	84.041
	16	89.969
2.115	1	148.11
	4	155.64
	16	185.76
4.233	1	125.73
	4	139.68
	16	183.44

the required currents for all loading conditions. Each figure has the three curves according to three gain values. Figures indicate that the required currents have fluctuations based upon required torques during the transients, and settle to the steady- state values.

#### D. THE REDUCTIONS OF THE REQUIRED TORQUE

The magnitudes of the required torques and required currents are related to the selection of size of the electrohydraulic actuator. The selections of the electrohydraulic actuator which depend upon the required torques and required currents, are also related to the weight, and cost. To reduce the required torques and required currents is very important in terms of the selection of the size of electrohydraulic actuator. In this research, a planned desired angle trajectory is used as the input replacing the step input.

The planned input is the combination of ramp and step function applied to the 4.233kg load with the position gain of 16. The initial point of the ramp function coincides with the initial angle of the flexible arm. The slope of the ramp function is selected as 2. Figure 4.16 shows the planned input of the desired angle as the combination function. Figures 4.17-4.19 show comparisons of the results between the step input and planned input. The difference of the maximum required torque for input functions is tabulated in Table 6.

Input Function	Max. Torque(N-m)
Step input	183.41
Planned Input	106.58

Table 6 indicates that the plan of the input function for the desired angle could result in the reduction of the maximum required torque and maximum required current. The total angle responses might be slower. We can expect different reductions of the required torques or required currents for same loading conditions and gain value when we change the input function of the desired angle.

#### E. THE REDUCTION OF VIBRATION

The system damping is considered to reduce the structural vibration. A damping ratio is applied to the small motion equation as follows;

$$M_{nq} \ddot{\theta} + M_{nn} \dot{V} + 2 \zeta W_n \dot{V} + K_n V = F_n$$

The no load fundamental frequency is predicted to be 2 HZ. A damping ratio(  $\zeta$ ) of 0.5 is applied to no load condition with the position gain of 2. Figures 4.20-4.23 show graphical results of the comparison of the no damping case with the damping case that has a 0.5 damping ratio. These result show that the movement of the end-point of the damping case is faster than the movement of the no damping. The system damping

yields the noticeable reduction of the vibration of small motion. The required torques of the system damping case show less fluctuations.

#### **F. THE ELECTROHYDRAULIC SATURATION**

The previous results for the required torques and required currents are for an ideal condition. When the electrohydraulic actuator is saturated at 15 milliamp current, all current exceeded 15 milliamp will be limited at 15 milliamp current. Figures 4.24-4.26 show the effect of the saturation for the 4.233 kg loading condition with the position gain of 16. The total angle responses with the saturated current show slightly slower movements compared to the ideal movement during transients. The required torques are also reduced due to the saturated current during the initial transients.

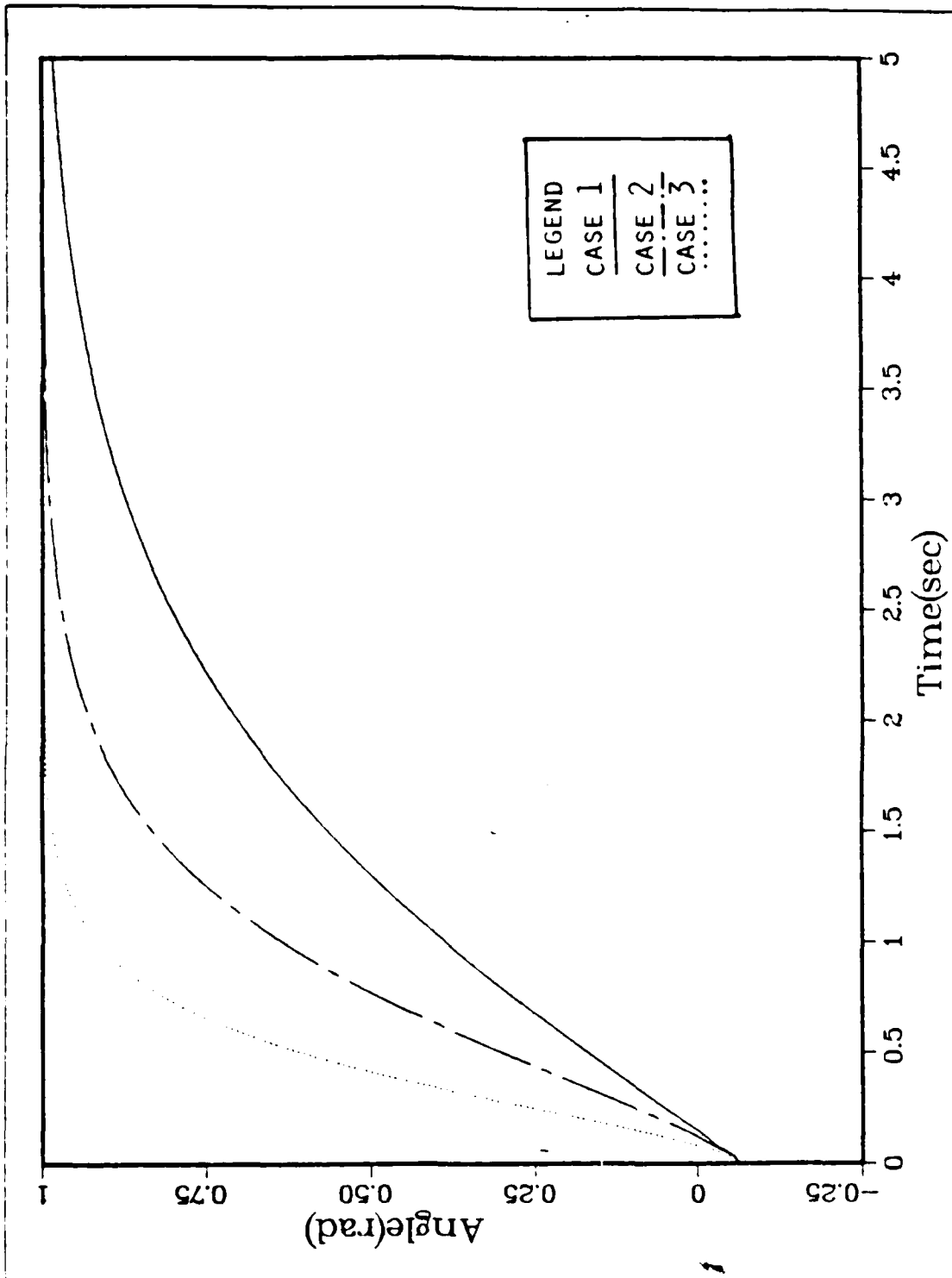


Figure 4.1 Total Angle Response ( 0 kg ).

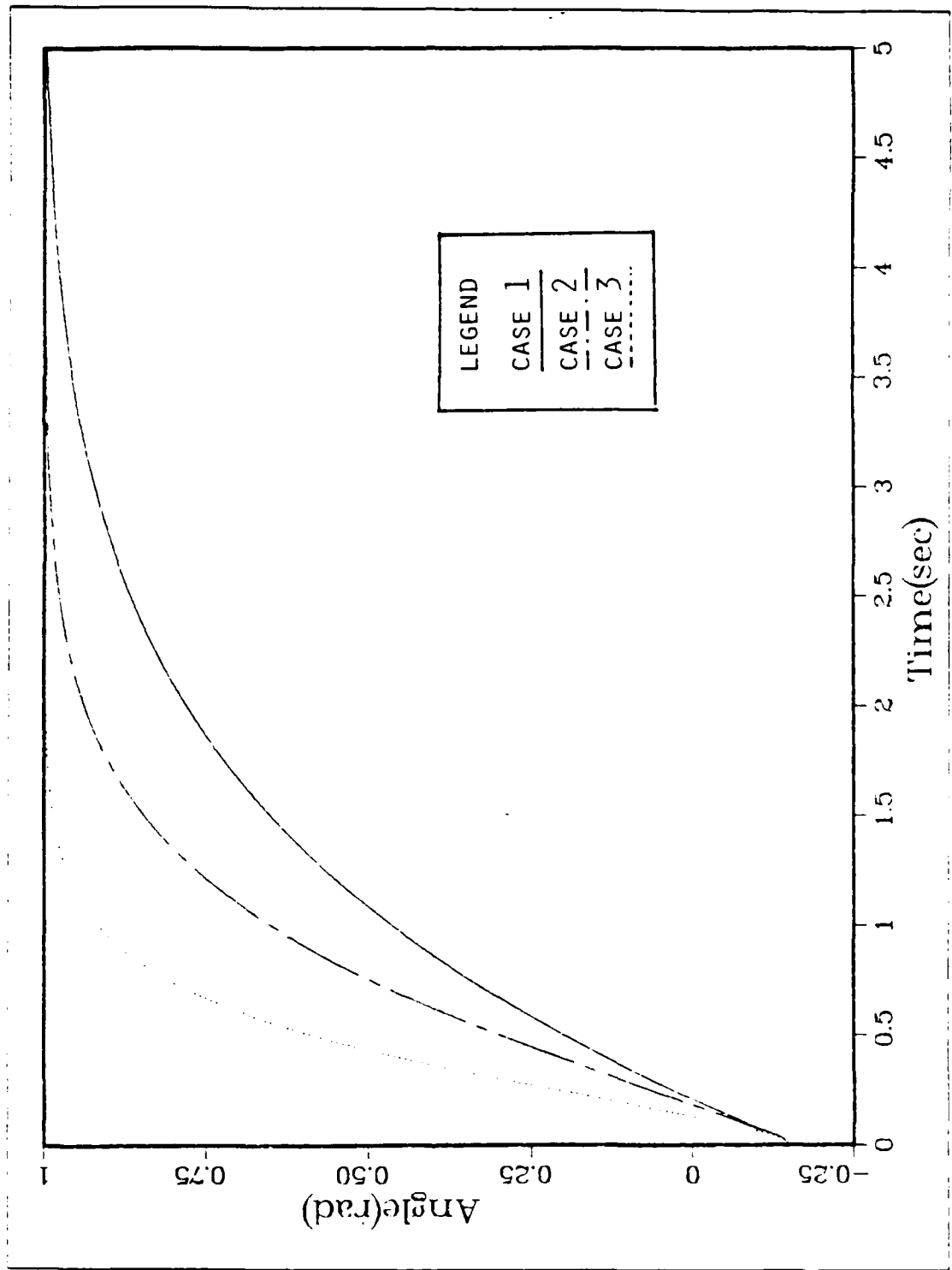


Figure 4.2 Total Angle Response ( 2.115 kg ).

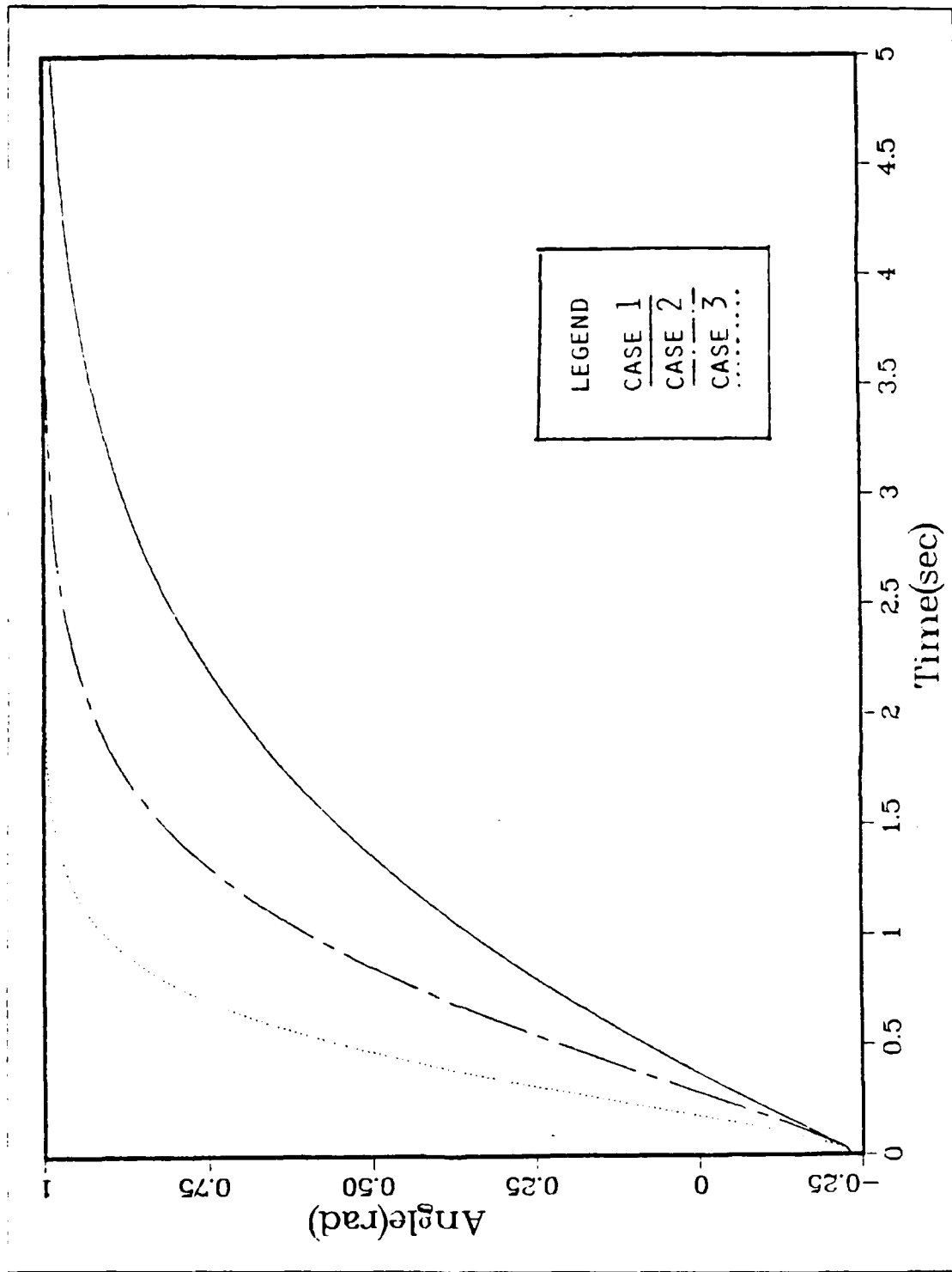


Figure 4.3 Total Angle Response ( 4.233 kg ).

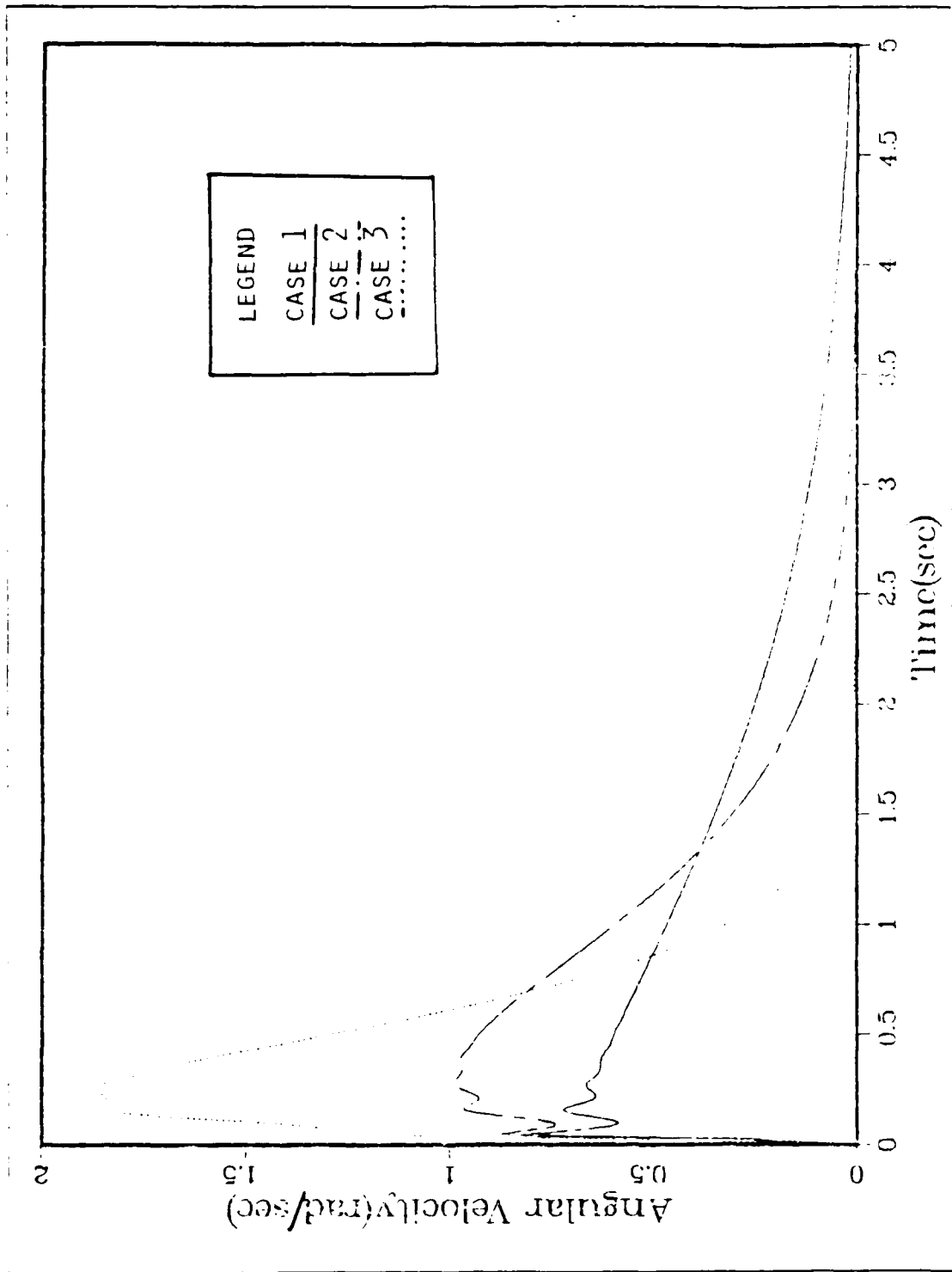


Figure 4.4 Total-Angle Velocity (4.233kg).

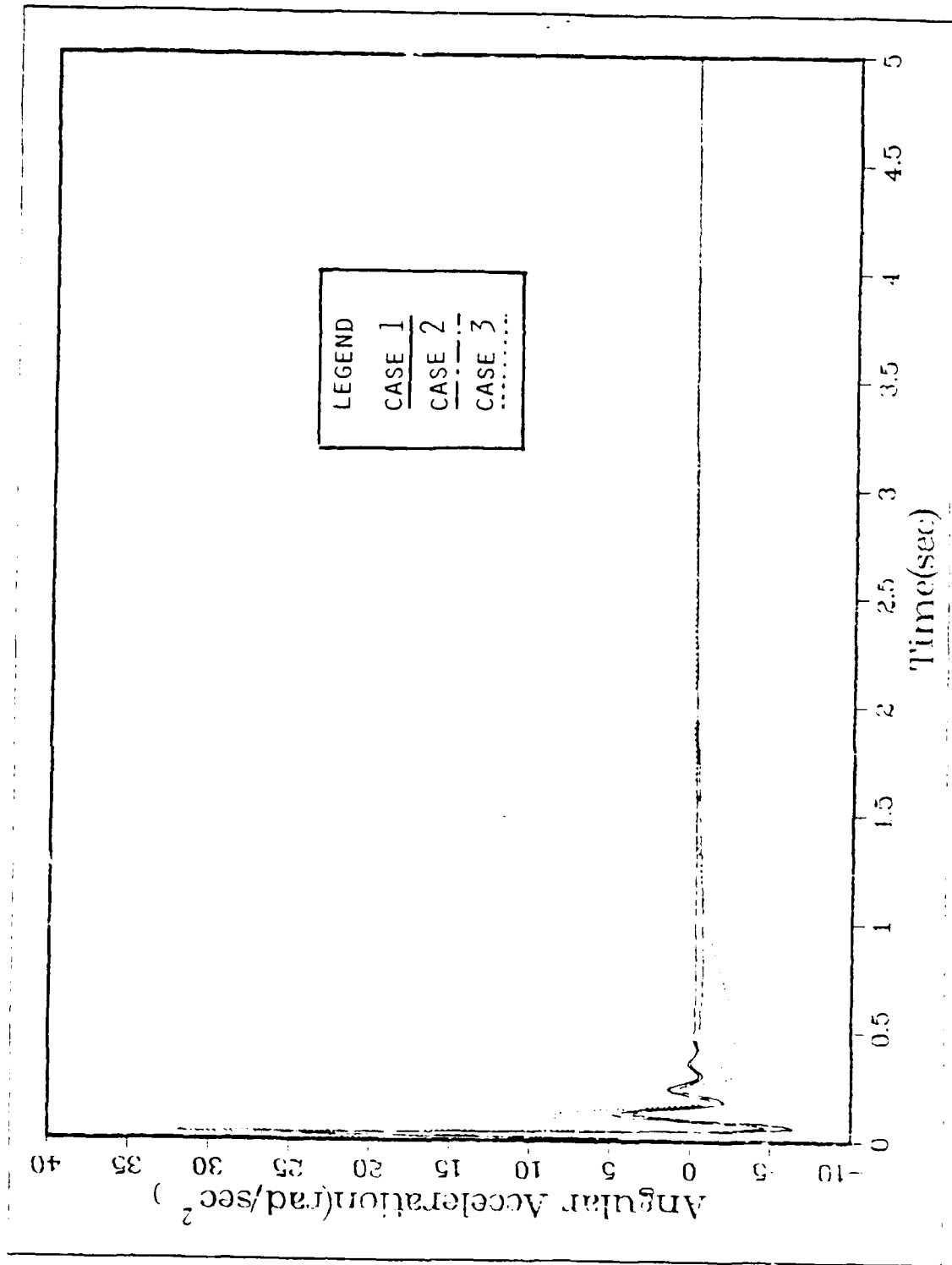


Figure 4.5 Total-Angle Acceleration 4.233kg.

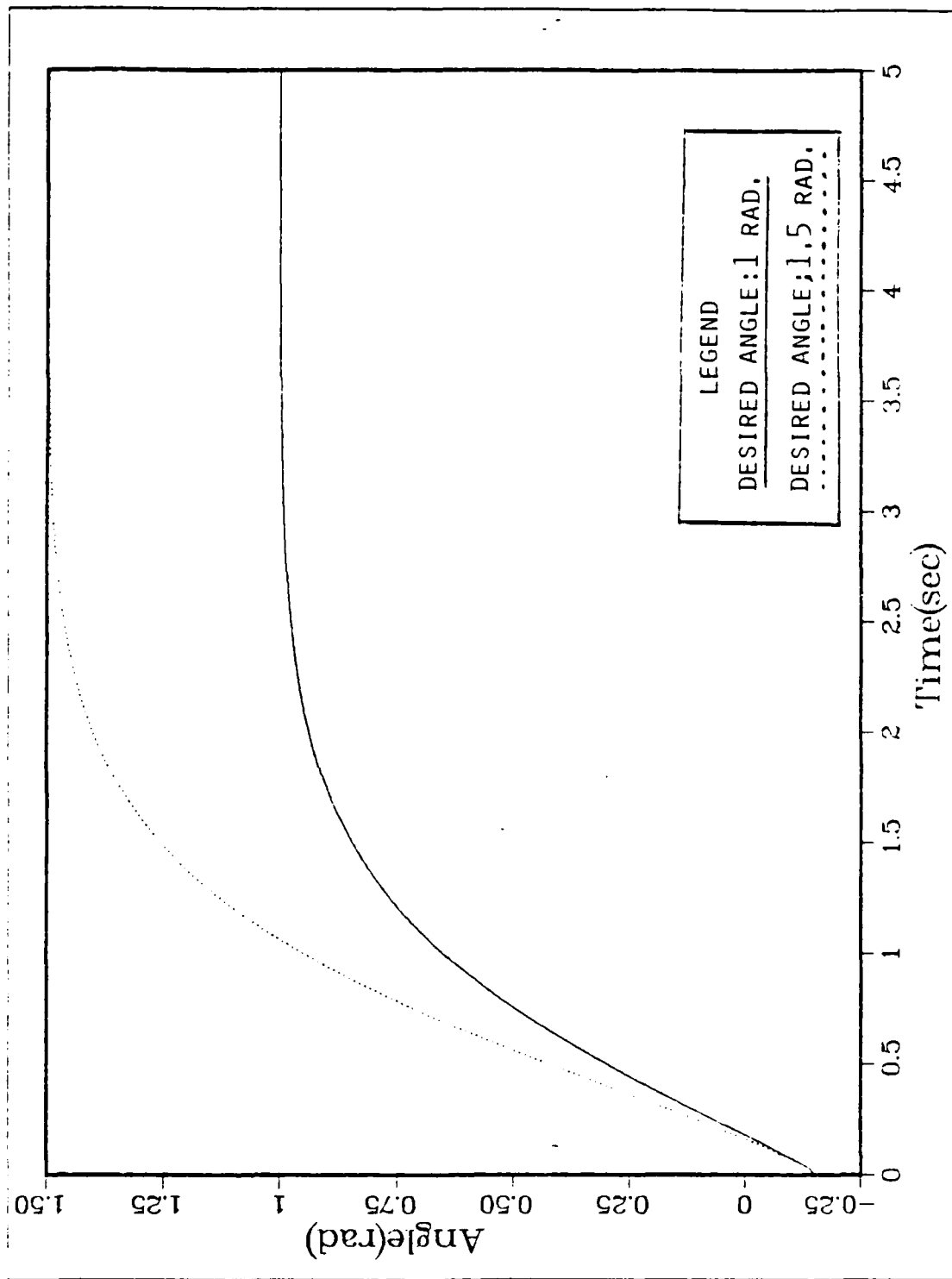


Figure 4.6 Total Angle Response for Various Desired Angles(2.115kg).

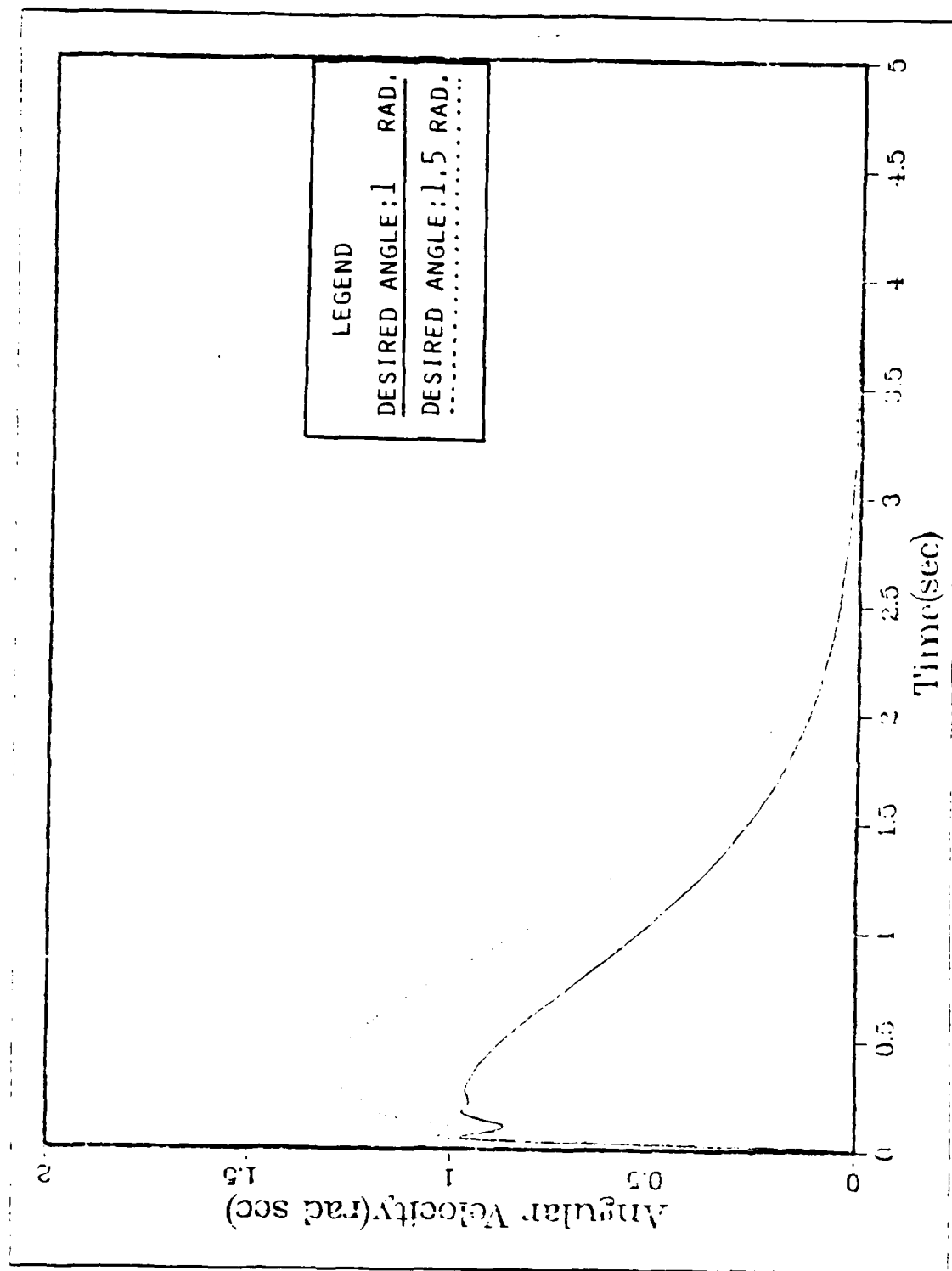


Figure 4.7 Total-Angle Velocities for Various Desired Angles(2.115kg).

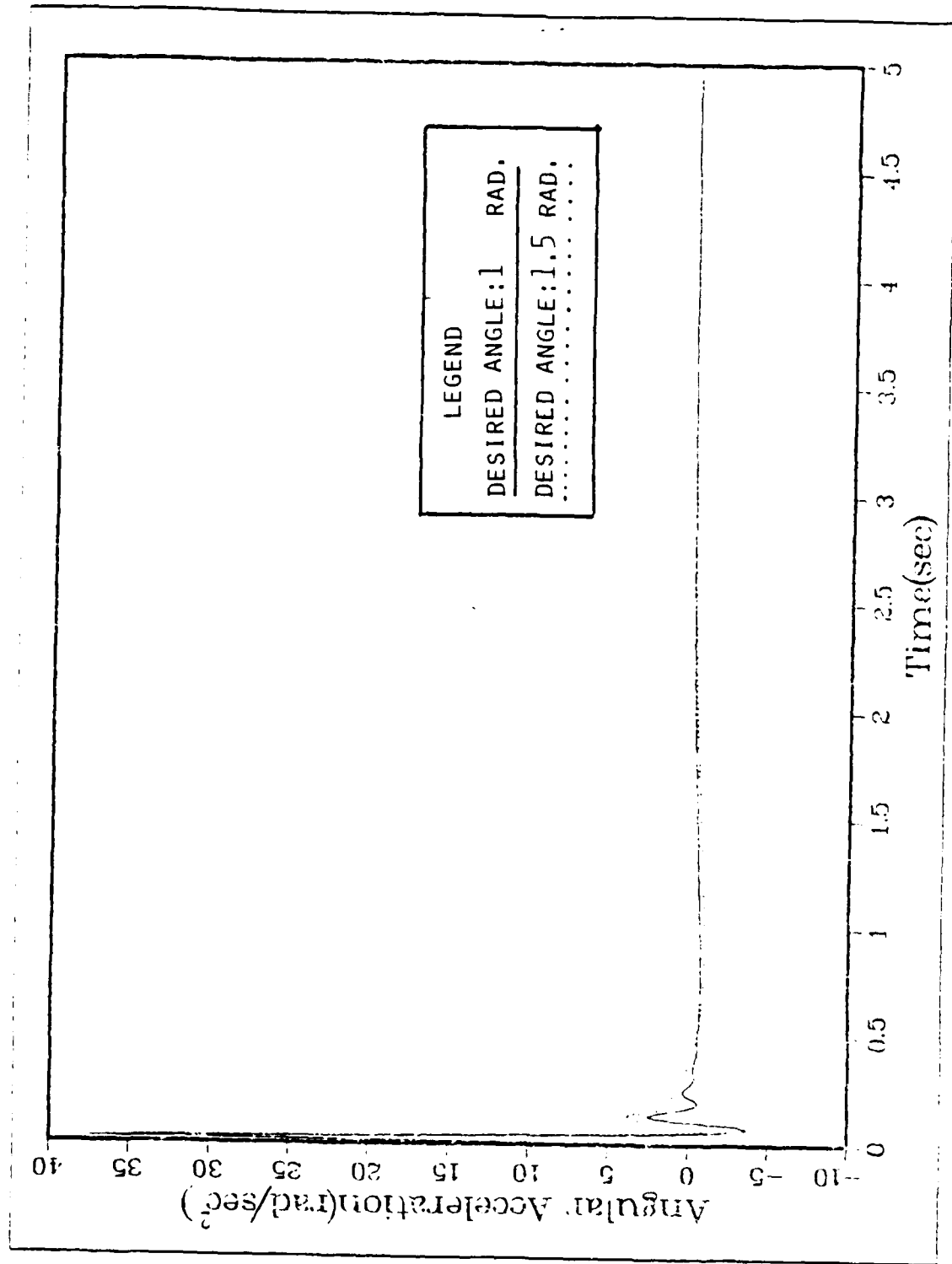


Figure 4.8 Total-Angle Accelerations for Various Desired Angles(2.115kg).

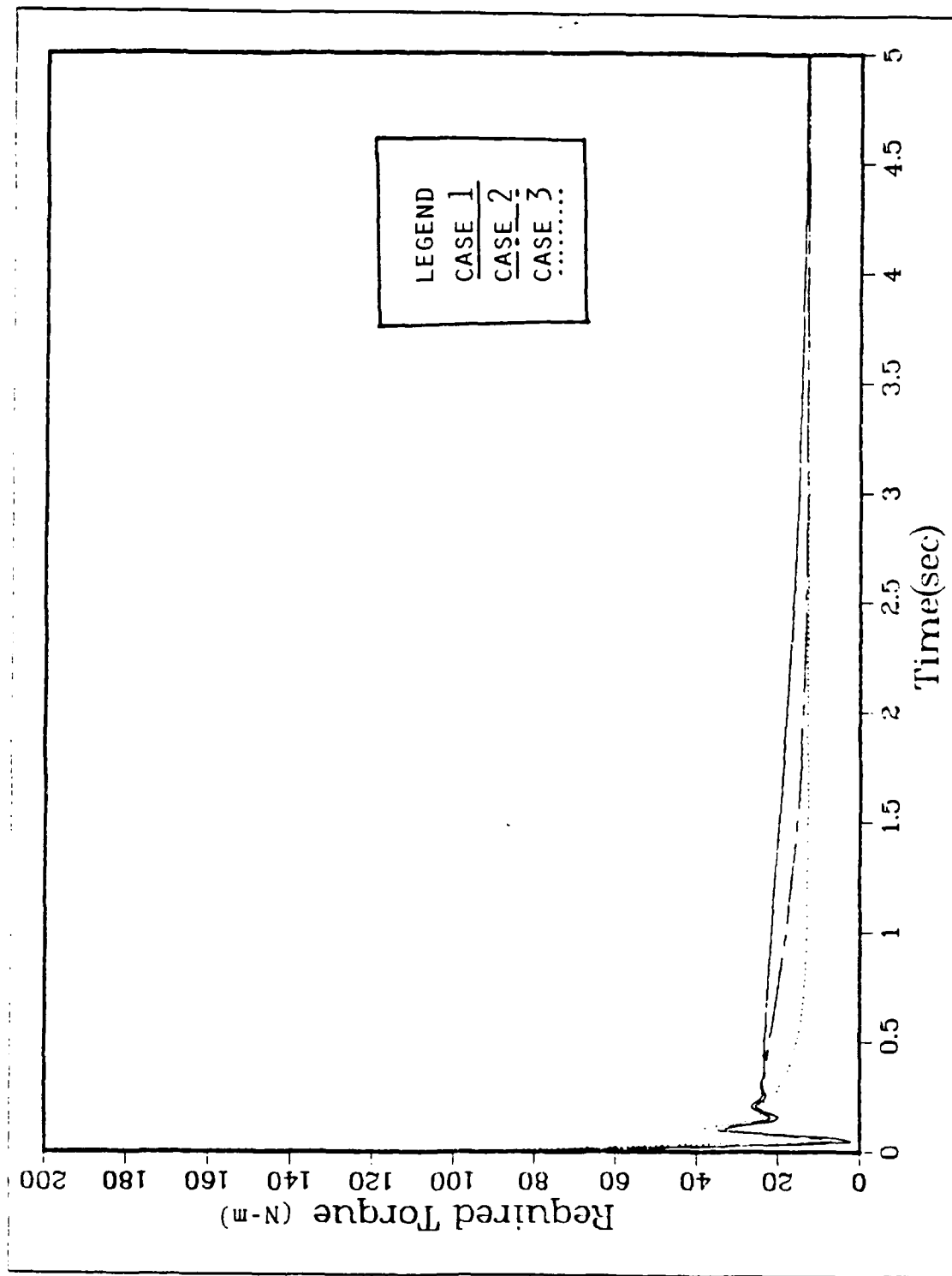


Figure 4.9 Required Torque ( 0 kg ).

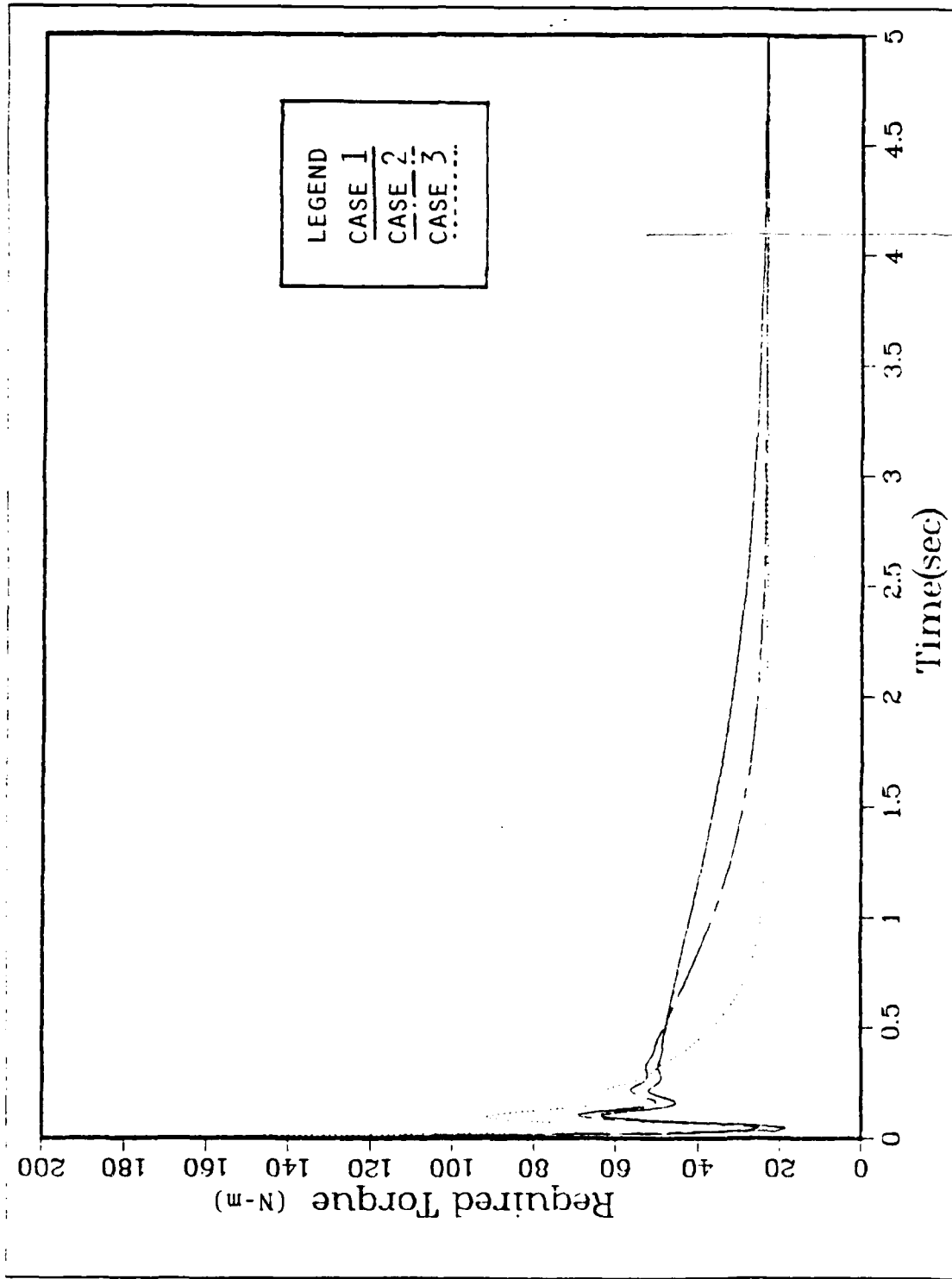


Figure 4.10 Required Torque ( 2.115 kg ).

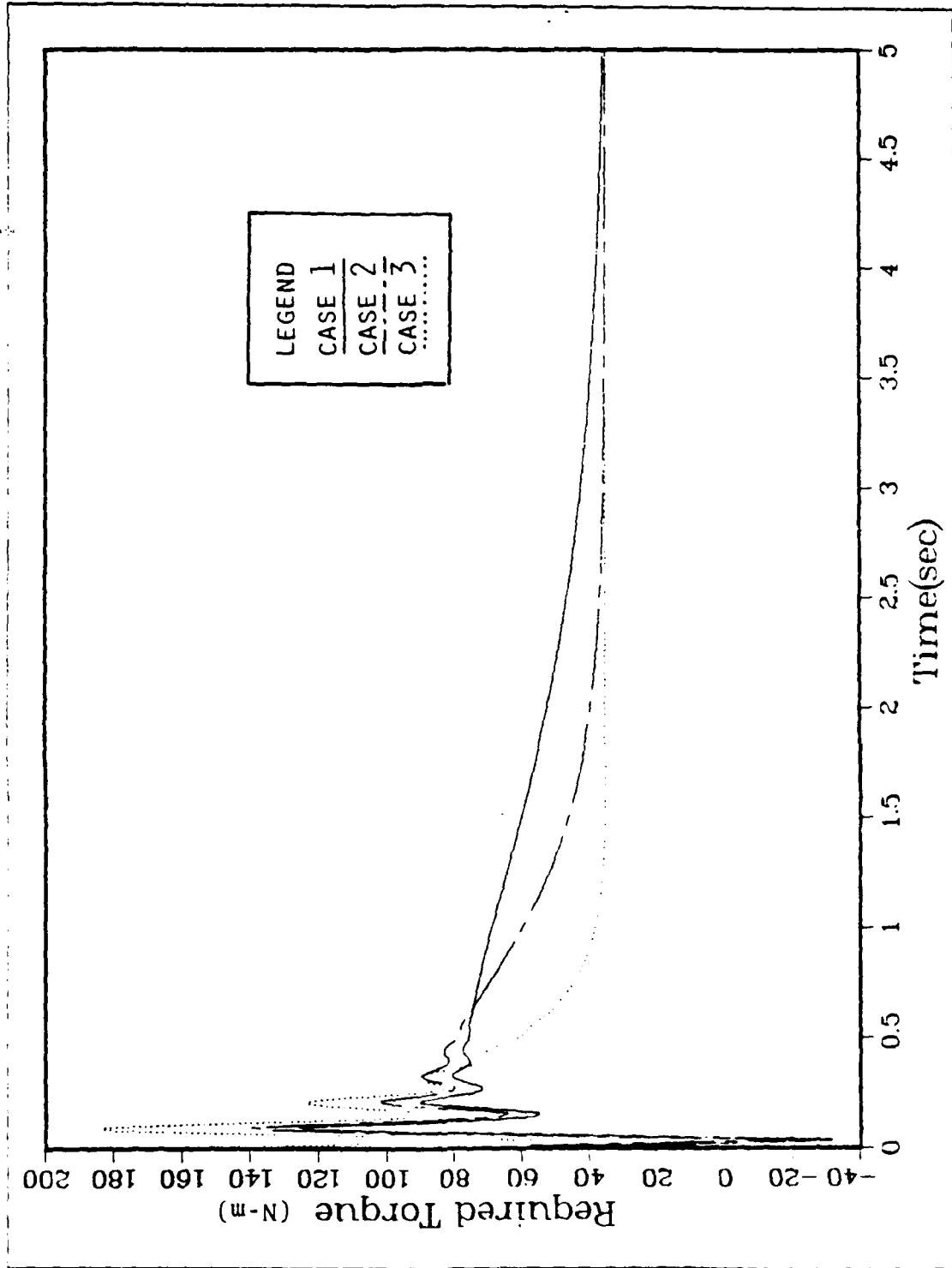


Figure 4.11 Required Torque ( 4.233 kg ).

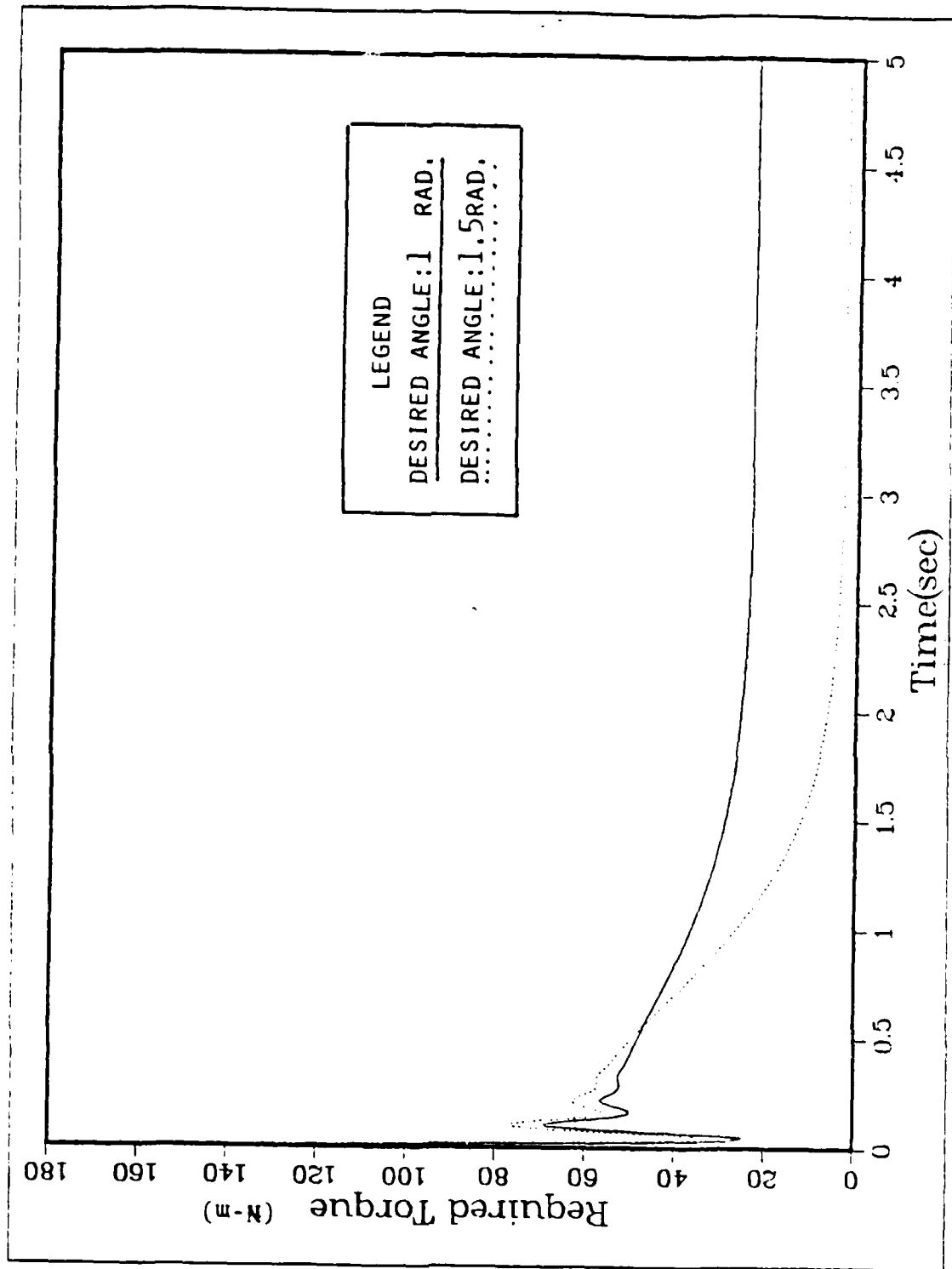


Figure 4.12 Required Torques for Various Desired Angles(2.115kg).

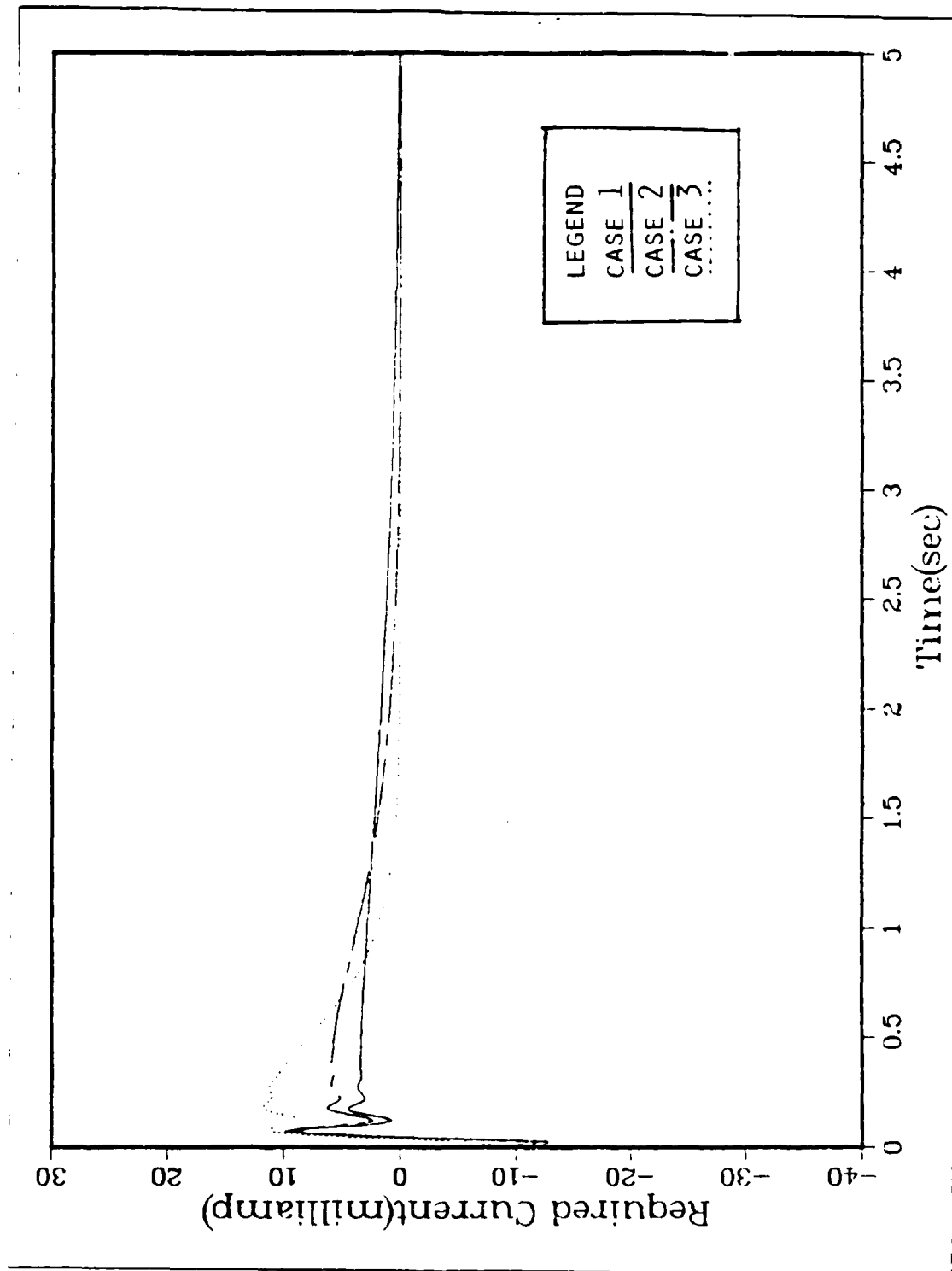


Figure 4.13 Required Current (0 kg ).

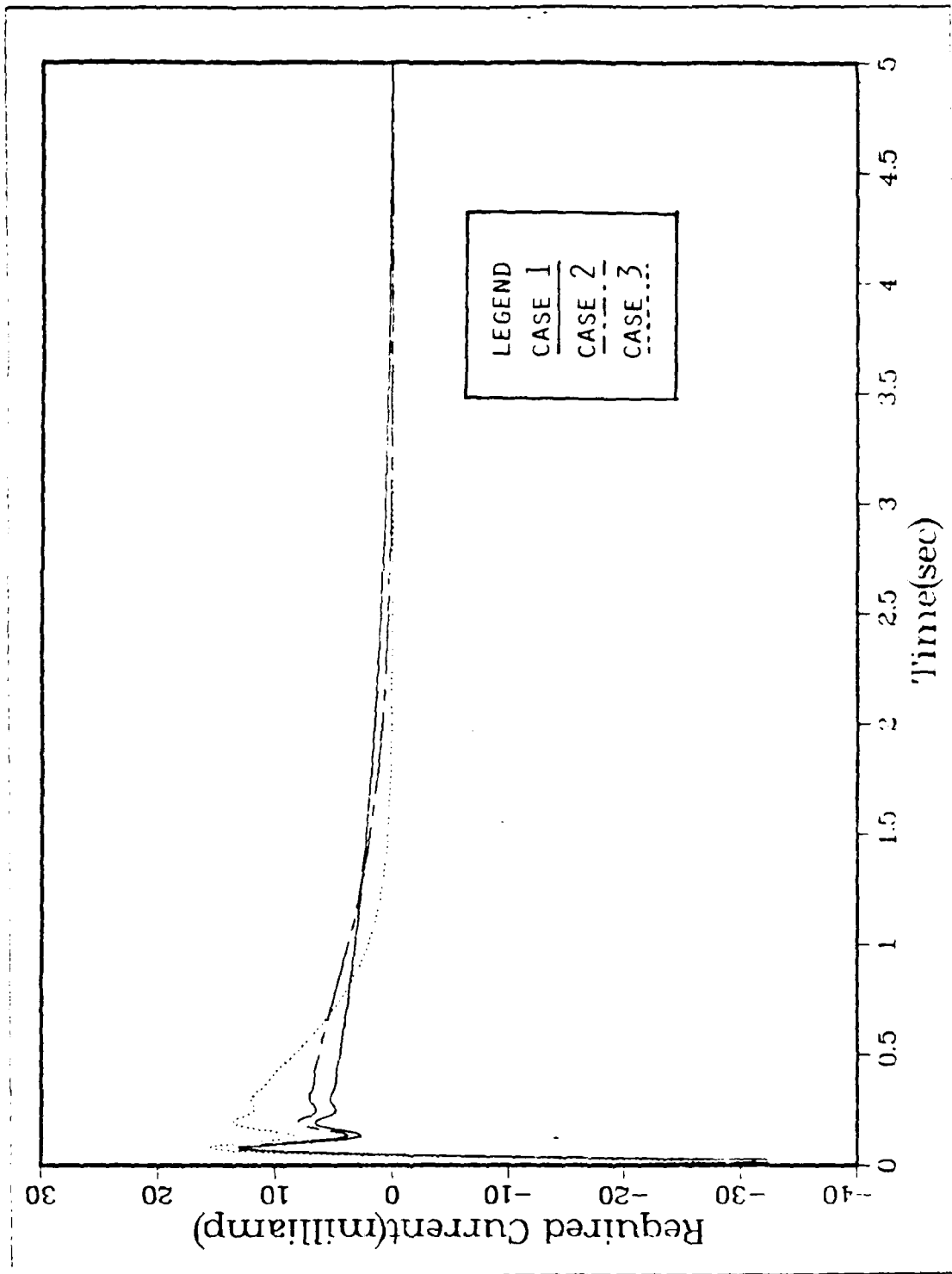


Figure 4.14 Required Current (2.115 kg ).

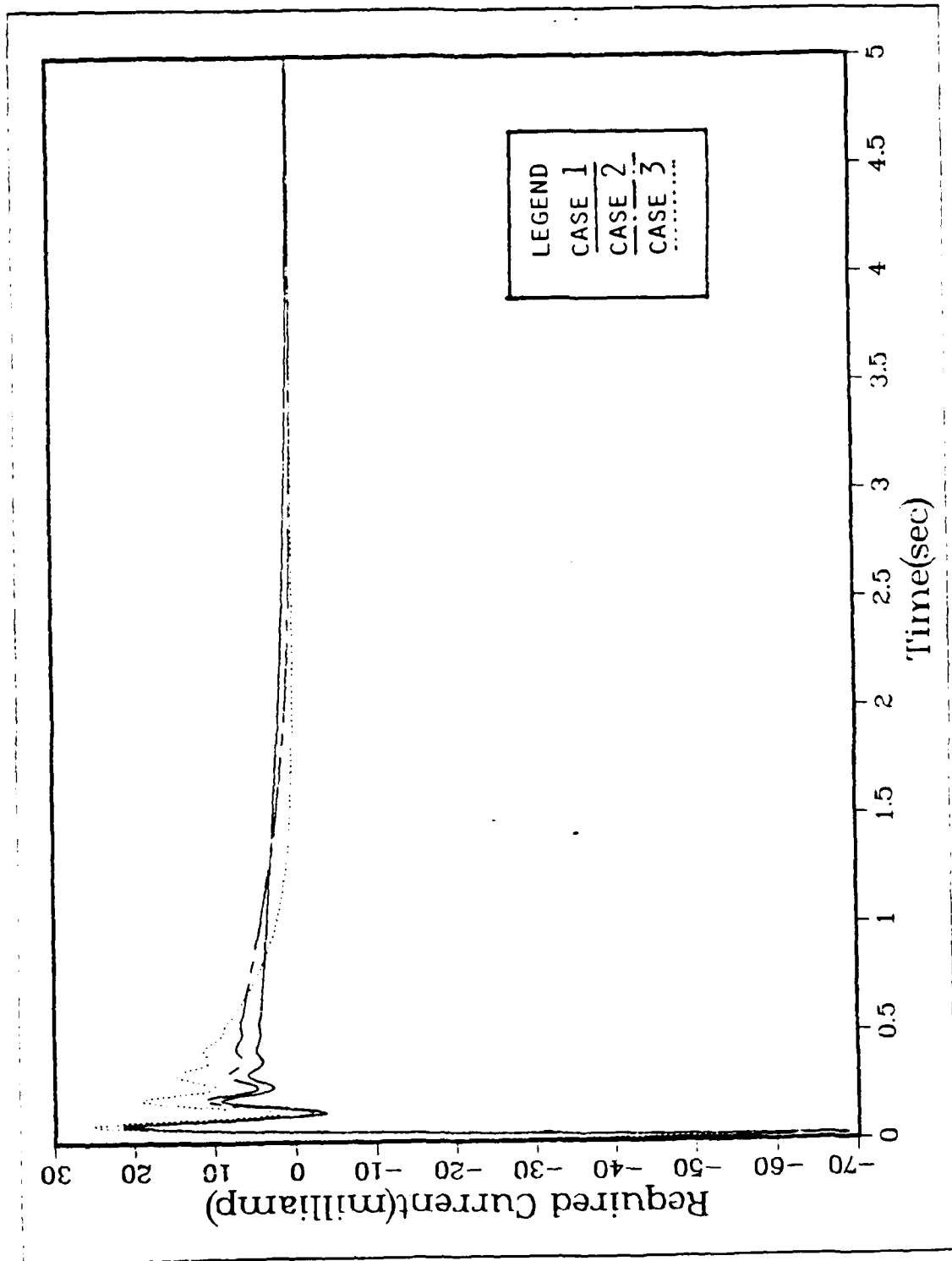


Figure 4.15 Required Current (4.233 kg ).

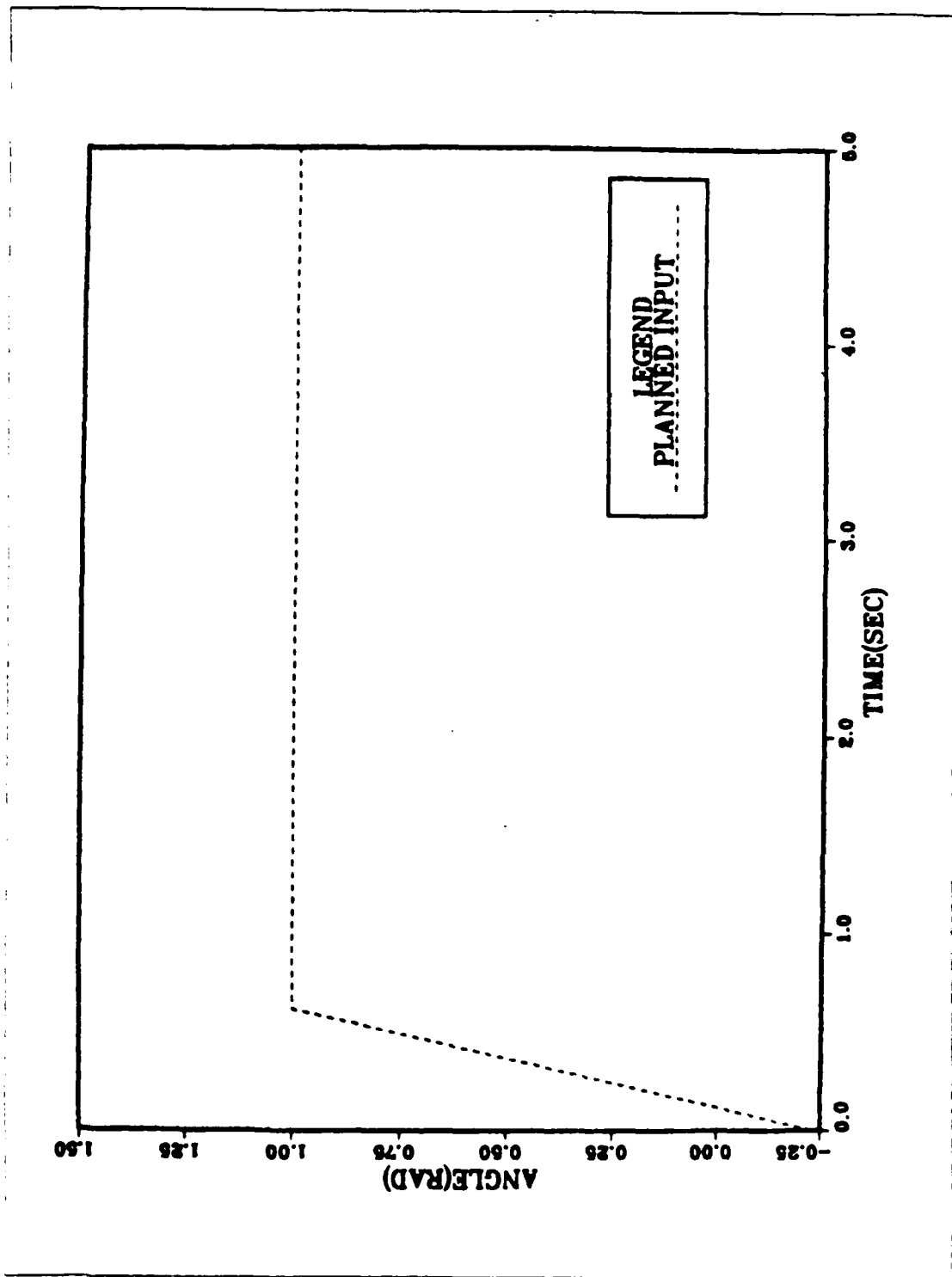


Figure 4.16 A Planned Input of the Desired Angle(4.233 kg ).

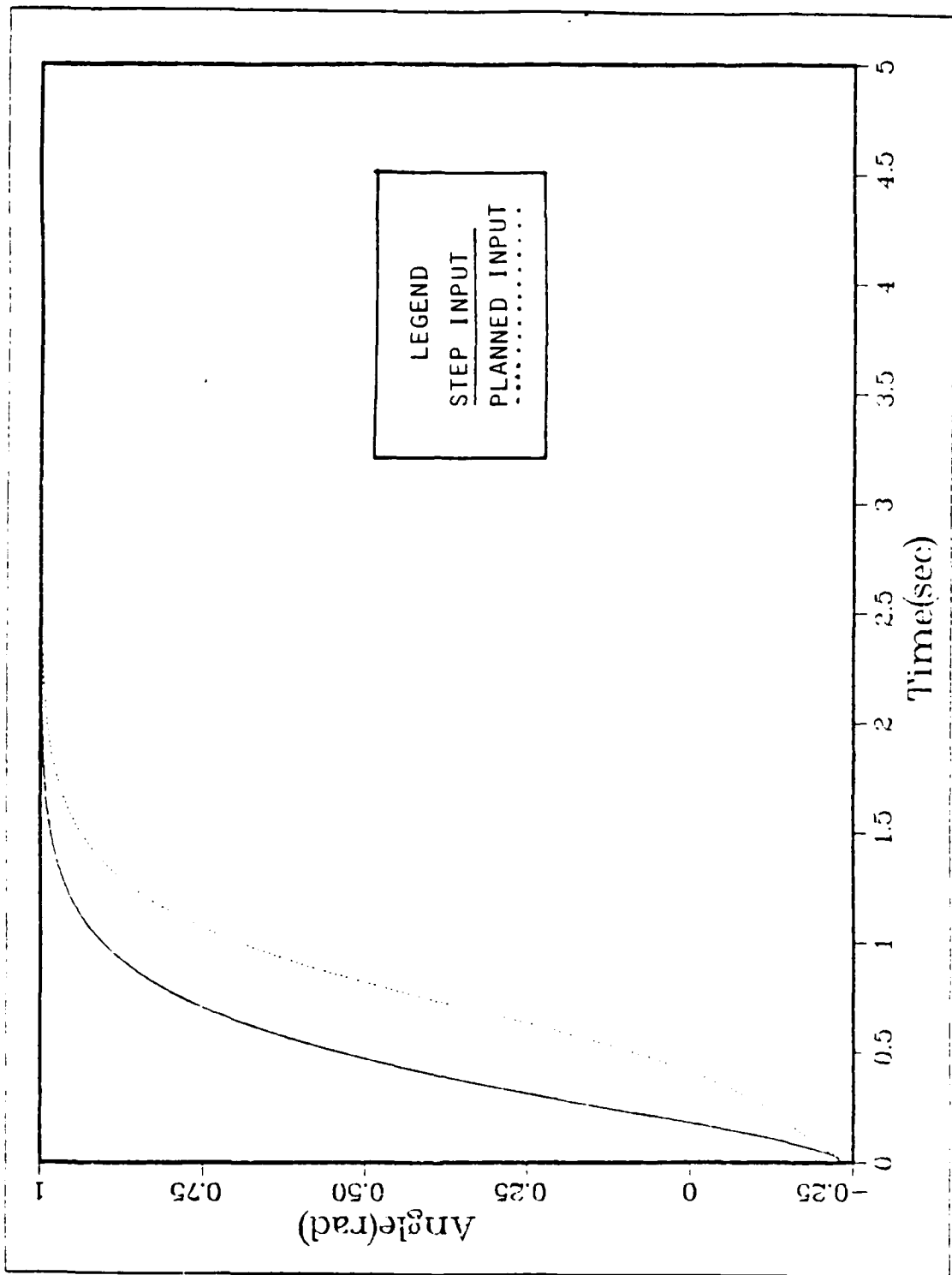


Figure 4.17 Total Angle Responses for Various Input Functions(4.233kg).

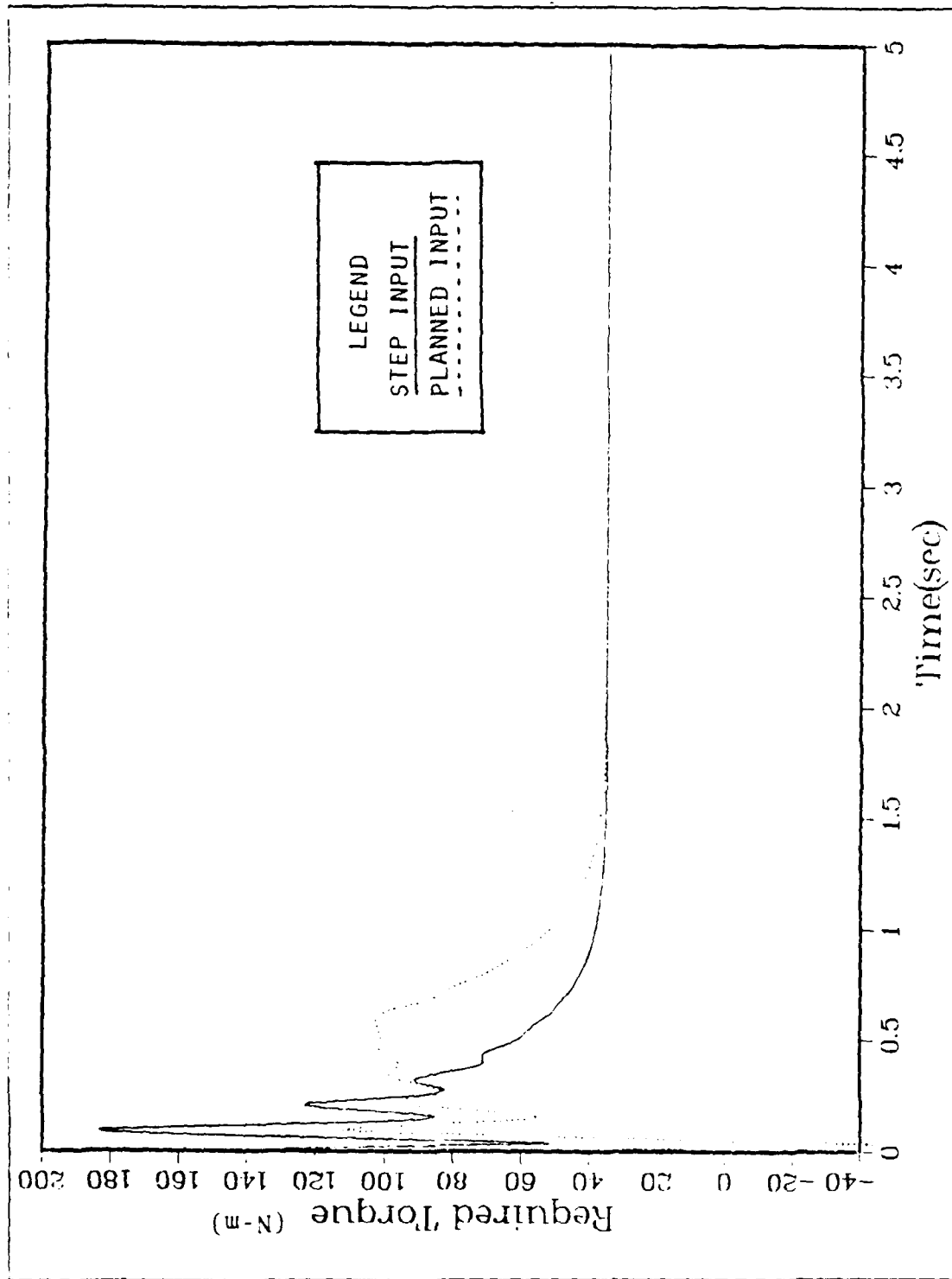


Figure 4-18 Required Torque for Various Input Functions(4.233 kg ).

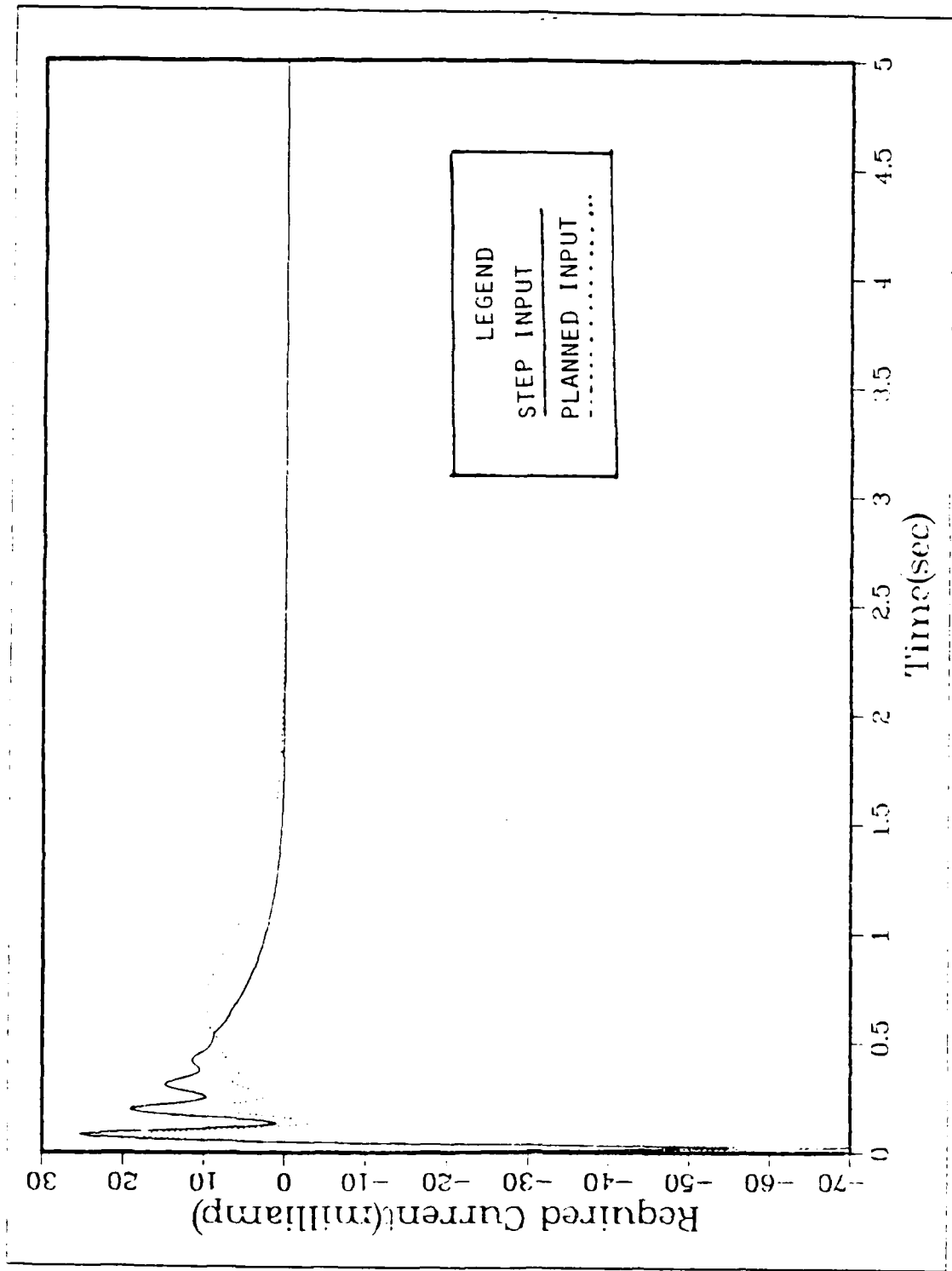


Figure 4.19 Require Current for Various Input Functions(4.233kg).

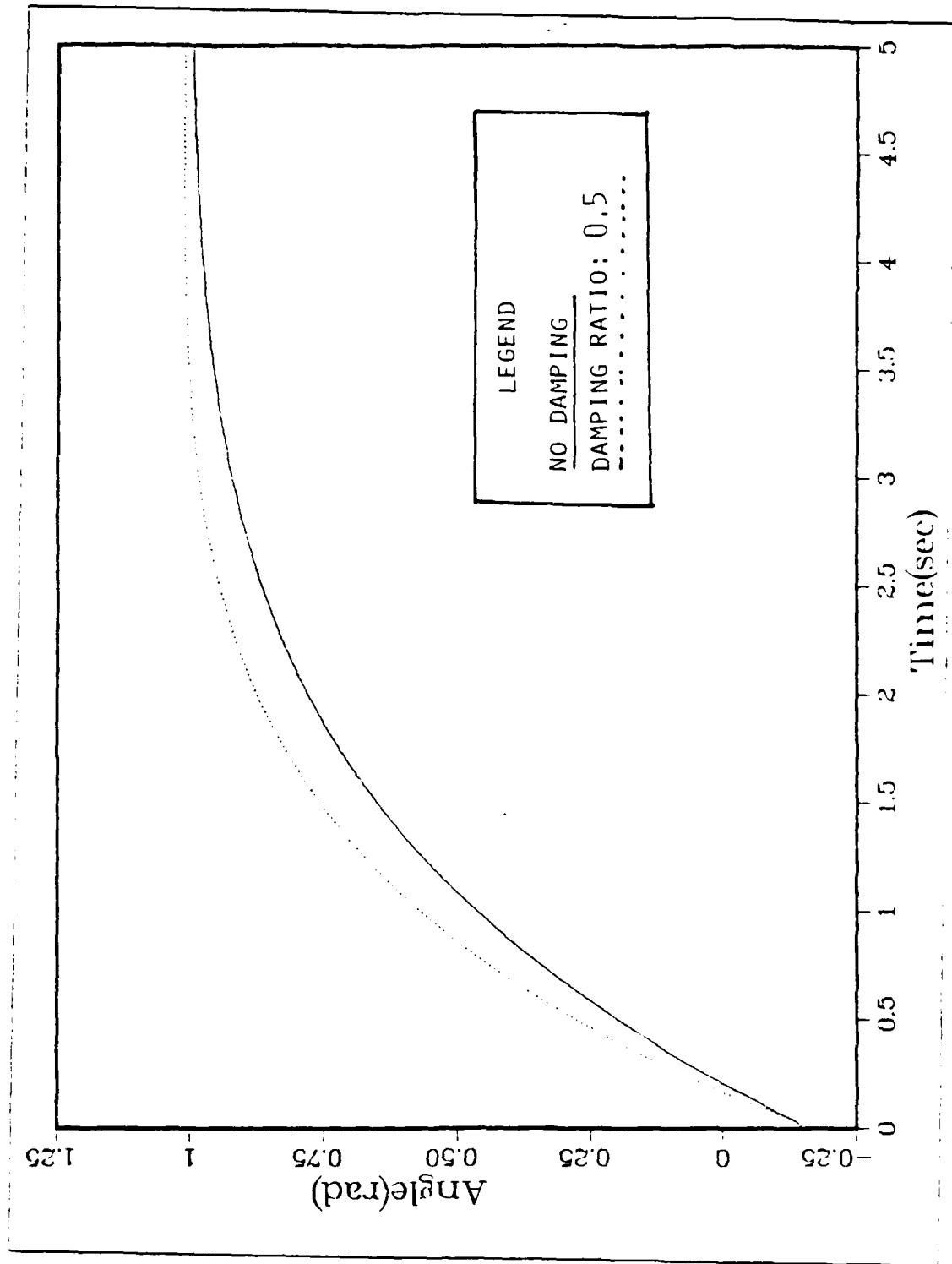


Figure 4.20 Total Angle Response for Various Damping Ratios(no load ).

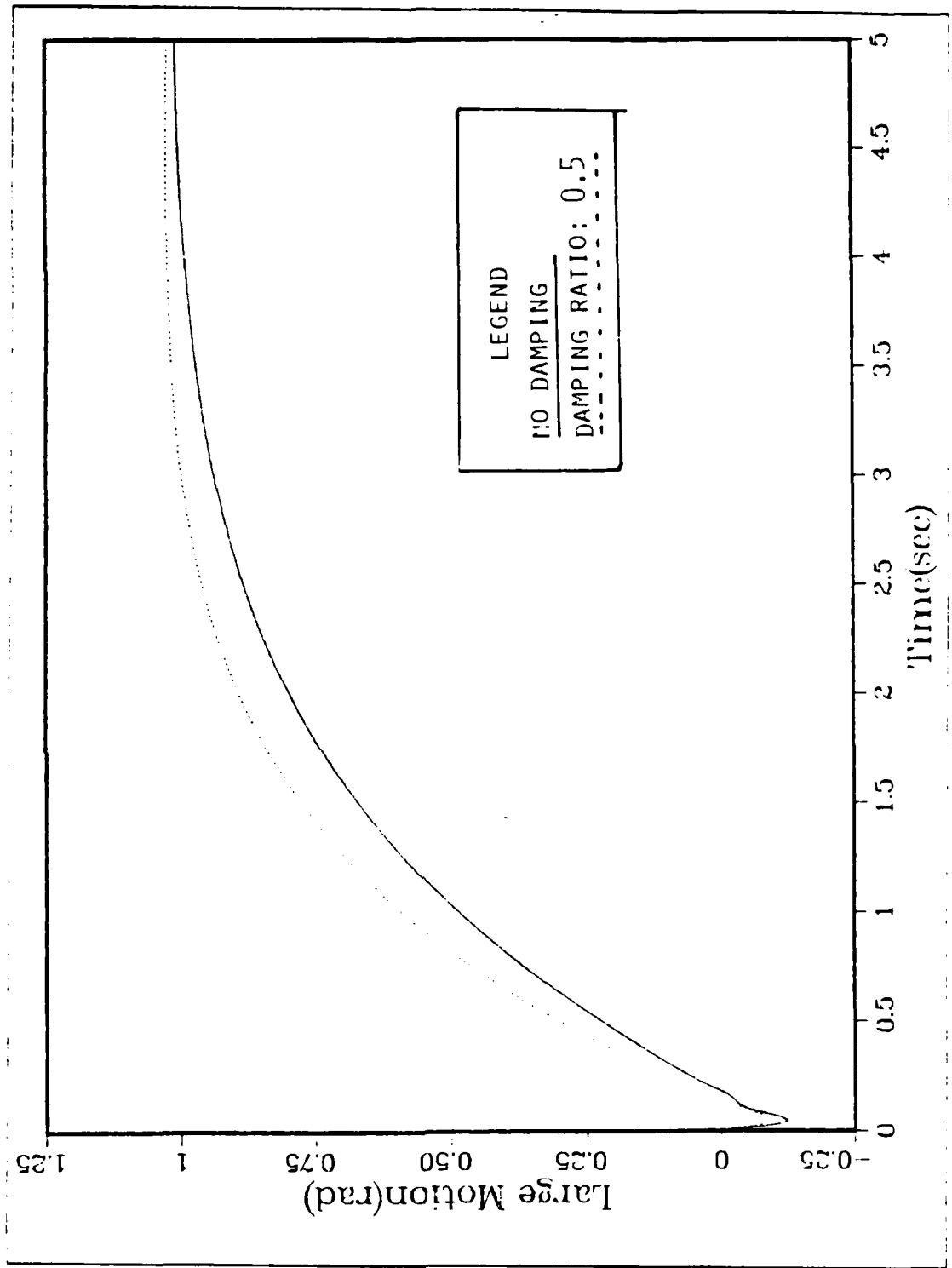


Figure 4.21 Large motion for Various Damping Ratios (no load ).

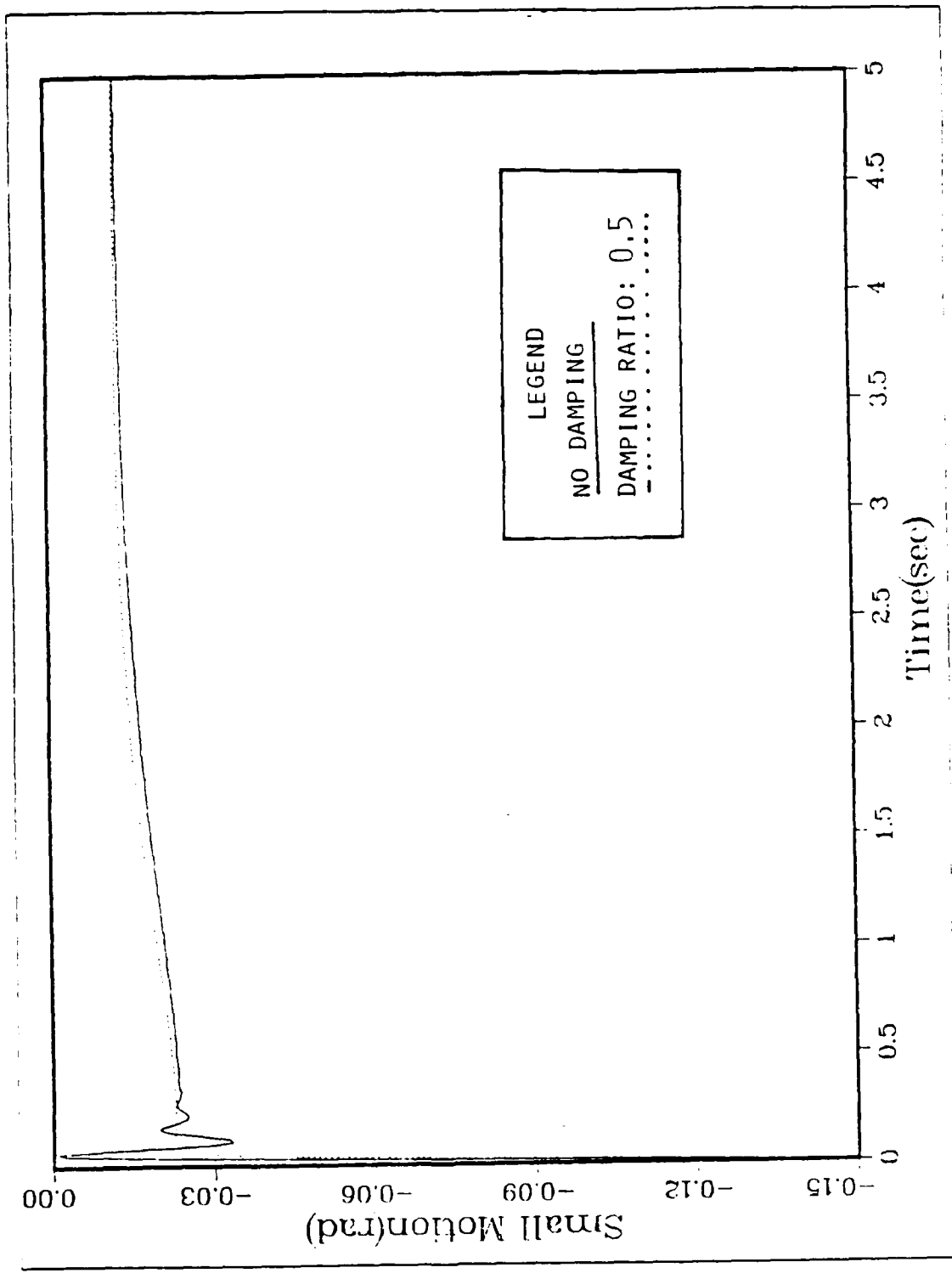


Figure 4.22 Small Motion for Various Damping Ratios (no load ).

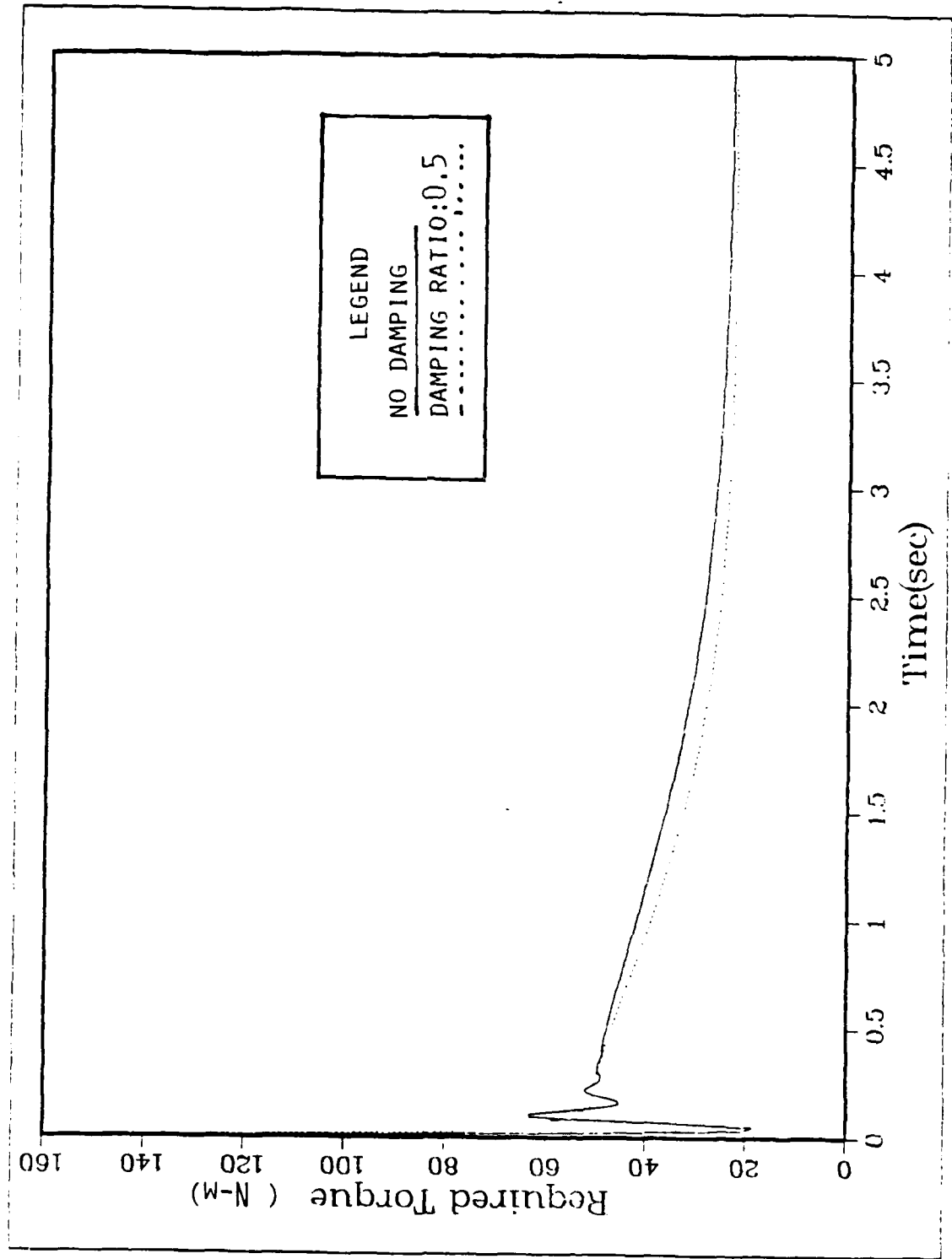


Figure 4.23 Required Torque for Various Damping Ratios (no load ).

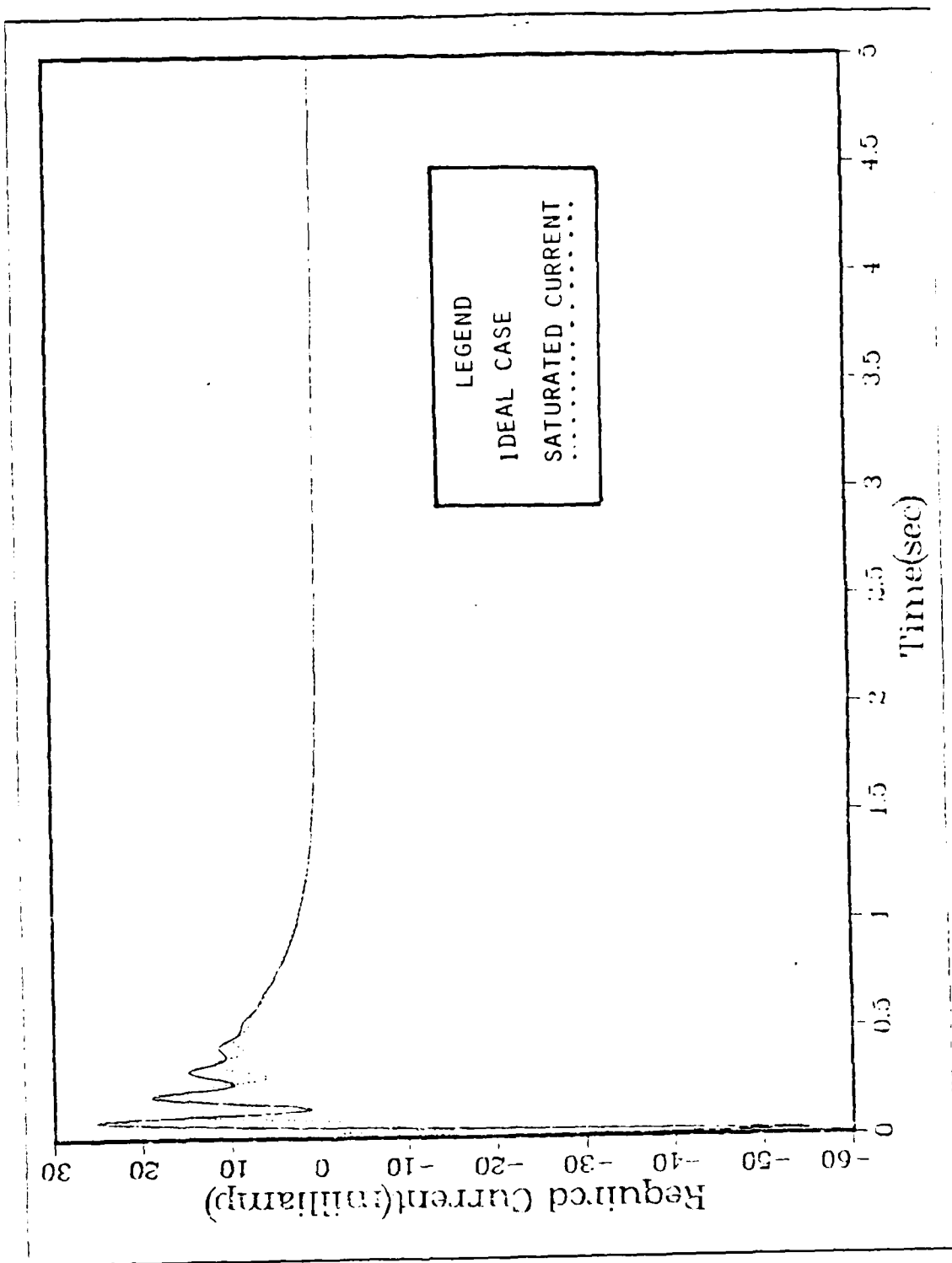


Figure 4.24 Required Currents for the Ideal and Saturated cases(4.233kg).

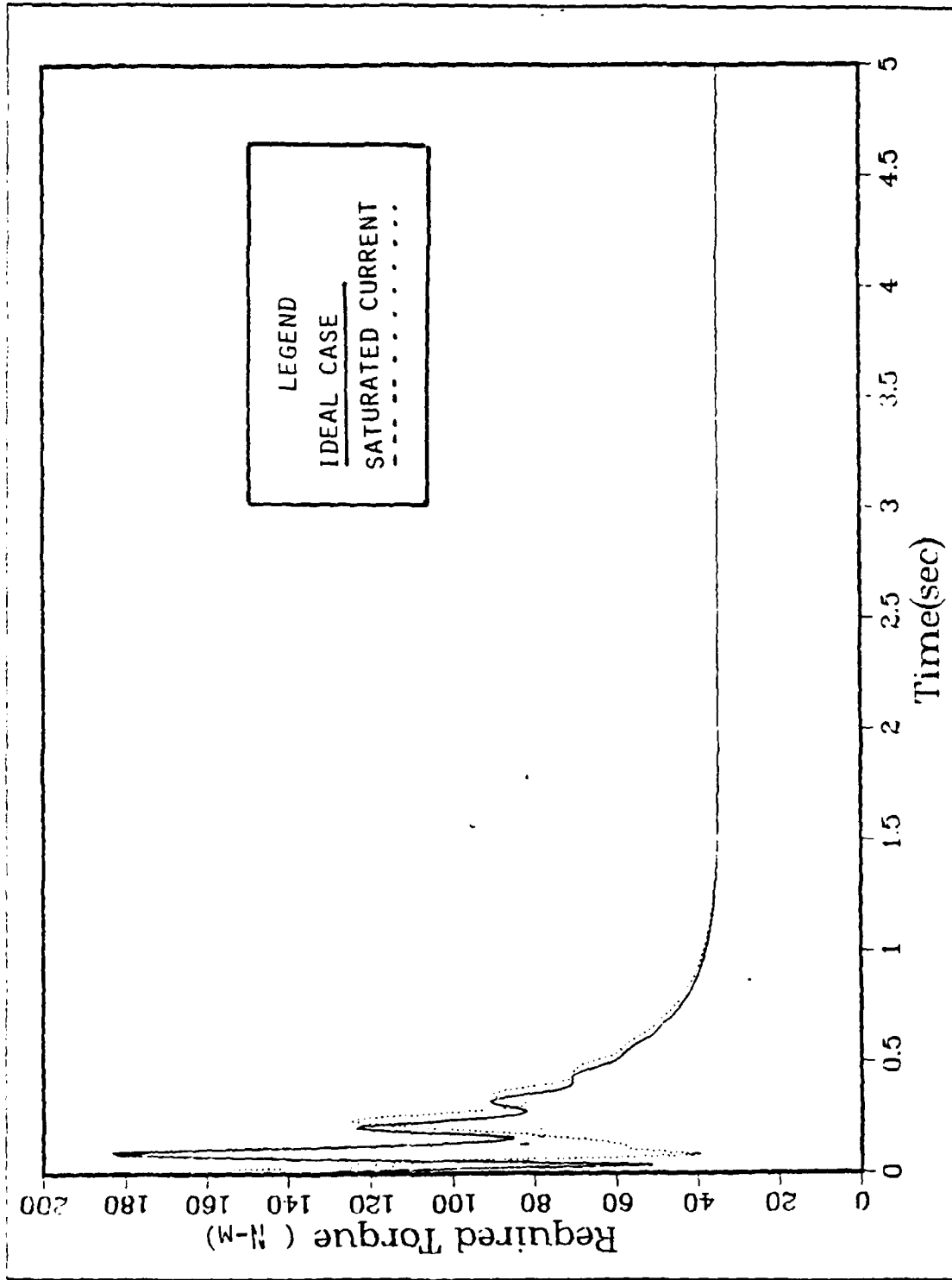


Figure 4.25 Required Torques for the Ideal and Saturated cases(4.233 kg ).

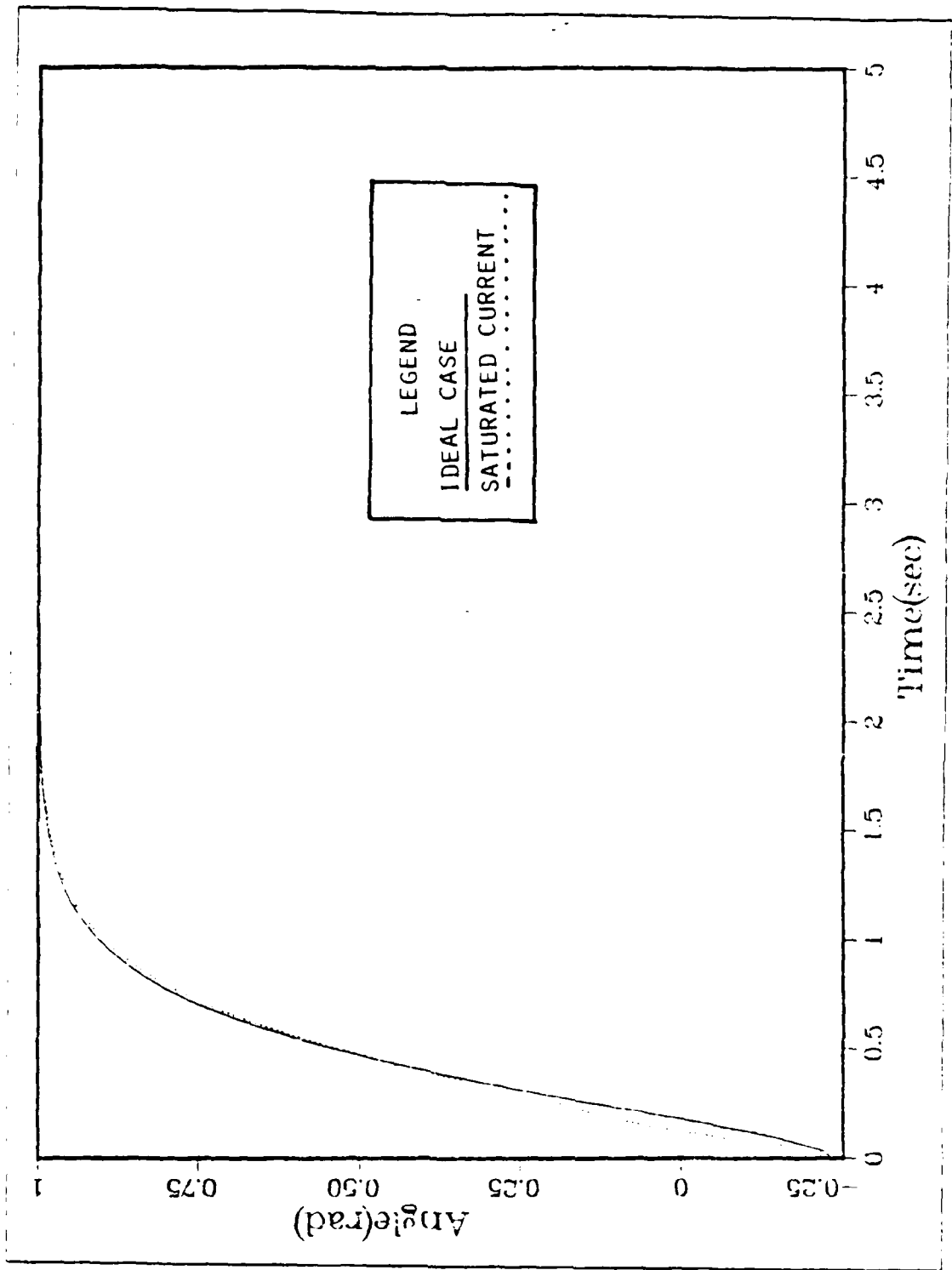


Figure 4.26 Total Angle Responses for the Ideal and Saturated cases(4.233kg).

## V. CONCLUSIONS AND RECOMMENDATIONS

### A. CONCLUSIONS

The purpose of this research is to design a controller for a single-link flexible manipulator using the Equivalent Rigid Link System. The control algorithm is formulated calculating the required torque to control the desired angle of the end-position. Comparisons of the system responses and required torques were made in the different conditions.

The results indicate that system responses and required torques are related to the selected gain values for all loading conditions. The movements of the end-point with higher gain values are faster to achieve the desired position. For different desired positions with the same gain, the end-point movements have the same pattern. These results indicate that non-linear motion is compensated in the control algorithm.

The required torques are increasing to deliver the load and overcome the inertial forces during transient times as gain values are increasing. The system rapidly settles to the steady state. Because of no steady state error, the required torques at the steady state have same values for the same desired positions even though the gains are different.

The maximum of the required torques and required currents are related to the capacity of the electrohydraulic actuator. The selection of size of electrohydraulic actuator affects the weight and cost of the control system. Since more demand is being placed on robot control with higher speeds and smaller actuators, it is important to reduce the maximum required torques and required currents. The application of the planned input of the desired angle as a combination of ramp and step functions lead a noticeable reduction of the maximum required torques and required currents. However, slower movements of the end-point are yielded during the transient period. The maximum required torques and required currents can be adjusted by the slope of the ramp function.

The results also indicate that the system damping provides a noticeable reduction of the structural vibration.

In addition, when the electrohydraulic actuator is saturated, the movement of the end-point is slower than the ideal case without saturation. The simulation serves an

useful method to run the physical plant within the operating limit of the selected electrohydraulic actuator.

## **B. RECOMMENDATIONS**

The long-term goal of this research is to design a controller being capable of achieving end effector positioning accuracy and stable movements. Simulation studies need to be continued for flexible multi-link system design using the ERLS model. In addition, the effects of the robustness and spillover problems need to be studied. Extension of the controller design and implementation to the multi-link of the ERLS model is eventually needed if the advantages of flexible manipulator is to be realized in practical industrial application.

## APPENDIX A

### DERIVATION OF THE EQUATIONS OF MOTION FOR THE SINGLE - LINK FLEXIBLE MANIPULATOR

The motion of the flexible link manipulator has been separated into large motions and small motions by the ERLS. The generalized coordinates are chosen to describe the large motions by the joint variable of ERLS and to describe the small motions by nodal displacements of link. The two generalized coordinates chosen are the rigid body rotation,  $\theta$ , and the nodal displacement,  $U(0)$  which can be measured at the end of the link. The following are the two sets Lagrange equations used to develop the equations of motion;

$$d/dt\{ \partial KE/\partial \dot{\theta} \} - \partial KE/\partial \theta + \partial PE/\partial \theta = F$$

$$d/dt\{ \partial KE/\partial \dot{U} \} - \partial KE/\partial U + \partial PE/\partial U = 0$$

where

KE - kinetic energy

PE - potential energy

$\theta$  - large motion joint variable measured between the ERLS link and the absolute x axis.

U - small motion displacement and slope

F - generalized force for large motion

The total kinetic energy is due to kinetic energy of the link motion  $(KE)_L$  and that of the actuators  $(KE)_a$ ;

$$KE = (KE)_L + (KE)_a$$

The actuator are much more rigid than the link, the actuator is treated as a rigid body and all kinetic energy terms are calculated separatly. Generalized forces include any applied force and damping forces. The expressions utilized for the determination of the kinetic energy of the system are as follows;

$$KE(\text{ arm }) = 1/2 \int_{\text{arm volume}} \mu \dot{\mathbf{R}}^t \{ \dot{\mathbf{R}} \} dv$$

$$KE(\text{load}) = 1/2 \text{Trace} \int_{\text{load volume}} \mu_L \dot{R}_L^t \{\dot{R}_L\} dv$$

$$KE(\text{rotor}) = 1/2 \text{Trace} \int_{\text{rotor volume}} \mu_r \dot{R}_r^t \{\dot{R}_r\} dv$$

The absolute position vector of the arm is determined from the following transformation;

$$R = W (r + D)$$

$W$  = the  $3 \times 3$  transformation matrix of function of  $\theta$ , only.

$r$  = the  $3 \times 1$  local position vector of the arm measured from the coordinate system whose origin is the end of the ERLS link.

$d$  = the  $3 \times 1$  deformation vector that only includes the transverse displacement, derivation of this vector is discussed in chapter 2.

$\mu$  = the mass density of the steel arm.

The absolute position vector of load is determined from the following transformation;

$$R_L = W D_L r_L$$

$D_L$  = the  $3 \times 3$  transformation matrix due to the local deformation of the arm tip.

$r_L$  = the  $3 \times 1$  local position vector for the load

$\mu_L$  = mass density of the steel load

The absolute position vector of the hydraulic actuator is given by the following transformation;

$$R_R = A_R r_R$$

$A_R$  = the  $3 \times 3$  transformation matrix due to the large motion rotation of the rotor

$r_R$  = the  $3 \times 1$  local position vector for the rotor

$\mu_R$  = the mass density of the actuator rotor, aluminum

Potential energy of the flexible arm comes from strain energy  $(PE)_d$  of the structure due to deformation and the gravitational energy  $(PE)_g$  of the system. The strain energy is produced by bending, torsion and extension. Along modeling, the lateral shear deflections are neglected so that the system energy of bending is due to flexure only. The expressions used for the determination of potential energy are as follows;

$$PE_d = 1/2 \int_{\text{link length}} E I_{zz} (v'')^2 dx$$

$$PE_g = - \int_{\text{link volume}} \mu r^t g dv$$

$$PE_{gL} = - \int_{\text{load volume}} \mu_L r^t g dv$$

where

$E I_{zz}$  = the flexural rigidity in the z direction, perpendicular to the plane of motion

$v''$  = second derivative of the transverse displacement V with respect to the local x coordinate direction expressed in terms of  $V(0)$

$g$  = gravitational acceleration vector

The following definitions for the inertia terms are utilized to simplify the computations and the resultant expressions in the equations of motion;

$$I_L = \text{the } 3 \times 3 \text{ inertia matrix of the load} \\ = \int_{\text{load volume}} \mu_L r_L r_L^t dv$$

$$I_R = \text{the } 3 \times 3 \text{ inertia matrix of the rotor} \\ = \int_{\text{rotor volume}} \mu_R r_R r_R^t dv$$

$$I_{111}(W_{\theta}^t, W_{\theta}) = \int_{\text{link volume}} \mu r^t W_{\theta}^t W_{\theta} r dv$$

$$I_{112}(W_{\theta}^t, W) = \int_{\text{link volume}} \mu r^t W_{\theta}^t W \Psi r dv$$

$$I_{121}(W^t, W_{\theta}) = \int_{\text{link volume}} \mu \Psi^t W_{\theta}^t W dv$$

$$I_{122}(W^t, W) = \int_{\text{link volume}} \mu \Psi^t W^t W \Psi dv$$

$$I_{122}(W^t, \ddot{W}_R) = \int_{\text{link volume}} \mu \Psi^t \dot{W}^t W_R \Psi dv$$

$$I_{122}(W_{\theta}^t, \dot{W}) = \int_{\text{link volume}} \mu \Psi^t W_{\theta}^t \dot{W} \Psi dv$$

$$I_{122}(W_{\theta}^t, W_{\theta}) = \int_{\text{link volume}} \mu \Psi^t W_{\theta}^t W_{\theta} \Psi dv$$

$$I_{yy} = \int \mu_L y^2 dv$$

$$I_{xx} = \int \mu_L x^2 dv$$

where

$\Psi$  = the  $3 \times 2$  link shape matrix

$W_{\theta}$  = derivative of the  $3 \times 3$  matrix  $W$  with respect to the joint variable  $\theta$

$\ddot{W}_R$  = result of the simplification of the second time derivative of the transformation matrix  $W$  and is termed the residual acceleration.

The following definitions are utilized to simplify the computations and the expressions used for computer coding of the equations of motion;

$$K_{11} = \int_{\text{link length}} \Gamma^t C \Gamma dx$$

$$H_{11} = \int_{\text{link volume}} \mu r^t dv$$

$$H_{21} = \int_{\text{link volume}} \mu_l \Psi^t dv$$

$$H_{41} = \int_{\text{link volume}} \mu_L r_L^t dv$$

$\Gamma$  = the second derivative of the shape function matrix

$C$  = the  $3 \times 3$  flexural rigidity matrix including only  $E I^{ZZ}$

The actual derivation of the equations of motion requires detailed, tedious substitution of the expressions for the kinetic energy and potential energy into the Lagrange equations, and the Lagrangian formulation yields two sets of equations. One set describes the large motions and the other set describes the small motions. These two sets of equations are non-linear, coupled, second-order, ordinary differential equations represented as follows;

$$M_{qq} \ddot{\theta} + M_{qn} \ddot{U} = F_q + \text{TORQUE}$$

$$M_{nq} \ddot{\theta} + M_{nn} \ddot{U} + K_n U = F_n$$

where

$M_{qq}$  =  $1 \times 1$  effective inertia matrix for large motions

$M_{qn}$  =  $1 \times 2$  coupled inertia matrix of the small motion effect on large motions

$M_{nq}$  =  $2 \times 1$  coupled inertia matrix of the large motion effect on small motions

$M_{nn}$  =  $2 \times 2$  effective inertia matrix for small motions

$K_n$  =  $2 \times 2$  stiffness matrix for small motions

$F_q$  =  $1 \times 1$  load vector for large motions

$F_n$  =  $2 \times 1$  load vector for small motions

- $\theta$  = generalized coordinate of the large motions  
 $U$  =  $2 \times 1$  generalized coordinate of the deformations representing the small motions-the displacement and slope.

The coefficients for the terms are defined as follows;

$$M_{qq} = I_{111}(W_{\theta}^t, W_{\theta}) + U^t I_{122}(W_{\theta}^t, W_{\theta}) U + \text{Trace}(W_{\theta} D_L I_L D_L^t W_{\theta}^t + A_R I_R A_R^t)$$

$$M_{qn} = I_{112}(W_{\theta}^t, W_{\theta}) + ((M_L L + M_x), (M_x L + I_{xx} + I_{yy}))$$

$$F_q = 2 U^t I_{122}(W_{\theta}^t, W) U + H_{11} W_{\theta}^t + U^t H_{21} W_{\theta}^t g - \text{Trace}(W_{\theta} D_L I_L D_L^t W_r + 2 W_{\theta} D_L I_L D_L^t W + A_R \theta I_R \ddot{A}_{RR}^t) + H_{11} D_L^t W_{\theta} g + T$$

$$M_{nq} = (\text{Trace}(W_{\theta} D_L I_L D_{L11}^t W^t), \text{Trace}(W_{\theta} D_L I_L D_{L12}^t W^t + I_{121}(W^t, W_{\theta}) + I_{121}(W^t, W_{\theta}))$$

$$M_{nn} = I_{122}(W^t, W) + M_L (\ddot{v}(0)) + (I_{xx} + I_{yy}) \times (\ddot{\phi}(0))$$

$$K_n = K^{11} + I_{122}(W^t, W_R)$$

$$F_n = H_{21} W^t g - (\text{Trace}(W_R D_L I_L D_{L11}^t W^t), + 2 W D_L I_L D_{L11}^t W^t), \text{Trace}(W_R D_L I_L D_{L12}^t W^t + 2 W D_L I_L D_{L12}^t W^t)) + H_{41} D_{L11}^t W^t g, H_{41} D_{L12}^t W^t g$$

where

$L$  = the arm length

$M_L$  = the mass of the load

$M_x$  = the first moment of the load with respect to the local y axis.

$T$  = the externally applied torque

$A_{RR}$  = a result of simplification of the second time derivative of the transformation matrix  $A_R$  and is termed  $D_{12}$  residual acceleration.

$A_R \theta$  = a derivative of  $A_R$  with respect to the joint variable theta.

$D_{L11}, D_{L12}$  = the derivatives of the arm tip deformation transformation matrix differentiated with respect to nodal deflection displacement and the nodal slope displacement respectively.

These expressions are coded and solved for in the computer program listed in Appendix B.



```

* 37.WTH-3X3 TRANSFORMATION MATRIX DIFFERENTIATED WITH RESPECT TO
* THETA
* 38.XIFRAC-VARIABLE FRACTIONAL AMOUNT OF INPUT CURRENT TO SERVO-
* VALVE
* 39.XIINP-CURRENT INPUT EQUAL TO INITIAL AND FRACTIONAL AMOUNTS
* 40.XIL-3X3 INERTIA MATRIX OF THE LOAD
* 41.XIO-INITIAL INPUT CURRENT TO SERVOVALVE
* 42.XIR-3X3 ROTOR INERTIA MATRIX
* 43.XK11- PARTIAL LINK STIFFNESS
* 44.XKN- LINK STIFFNESS
* 45.XKV-SERVOVALVE SIZING CONSTANT
* 46.XLL-LENGTH OF FLEXIBLE ARM
* 47.XML-MASS OF LOAD
* 48.XMNN-COEFFICIENT OF SMALL MOTION ACCELERATIONS IN THE
* SMALL MOTION DYNAMIC EQUATIONS
* 49.XMNO- COEFFICIENT OF LARGE MOTION ACCELERATIONS IN THE
* SMALL MOTION DYNAMIC EQUATIONS
* 50.XMON- COEFFICIENT OF SMALL MOTION ACCELERATIONS IN THE
* LARGE MOTION DYNAMICS EQUATION
* 51.XMOO-COEFFICIENT OF LARGE MOTION ACCELERATION IN THE LARGE MOTION
* DYNAMICS EQUATION
* 52.XMOOP- DUMMY MATRIX FOR USE IN FORMULATING THE EQUATIONS OF
* MOTION
* 53.XMR-MASS OF ACTUATOR ROTOR
* 54.XMU-MASS DENSITY OF STEEL FLEXIBLE ARM
* 55.XMX-FIRST MOMENT OF LOAD WITH RESPECT TO THE LOCAL COORDINATE
* Y AXIS
* 56.ZI-AREA MOMENT OF INERTIA OF FLEXIBLE ARM
* 57.TAG- TOTAL total angle
* 58.TAG1- TOTAL ANGULAR VELOCITY
* 59.TAG2- TOTAL ANGULAR ACCELERATION
* 60.RETO- REQUIRED TORQUE
* 61.REIC -REQUIRED CURRENT

```

INITIAL

```

*
* INITIAL VALUES OF PARAMETERS ARE INPUTTED VIA XINIT SUBROUTINE
*

```

```

D DIMENSION U( 1),XMOO(1),XMOOP(1 ),DL1(3,3),WTH(3,3),ARTH(3,3),
D #XIR(3,3),XMON(1 ),UD(1 )HI1(1,3),G(3,1),H21(1,3),
D #WRDD(3,3),DL1D(3,3),WD(3,3),ARRDD(3,3),H41(1,3),XK11(1 ),
D #XMNO(1 ),W(3,3),XMNN(1 ),XKN(1 ),FN(1 ),BIGM(2,2),
D #BIGF(2,1),XIL(3,3),DL11(3,3),DEFMD(1),SOL(2),THD(1),
D #A(1),E(1),ZI(1),FO(1),GPOS(3),XITH(1),
D #XMU(1),XLL(1),XML(1),XMR(1),XMX(1),TH(1),TORQUE(1),DEFM(1),
D #PS(1),CTM(1),VT(1),BE(1),DM(1),XKV(1),TE(1),
D #QL(1),PL(1),DIFF(1),XIINP(1),QERR1(1),QERR(1),FACTOR(1),
D #REIC(1),RETO(1),FTT(1),CTB(1),FCO(1),
D #DEQ(1),DI(1),DEPL(1)

```

FIXED I

NOSORT

```

D COMMON/FCDATA/C1,C2, A1P,A2P,BETA1,BETA2

```

```

C1=0.515462194
C2=-0.205906794
A1P=1.362220557
A2P=0.981867539
BETA1=1.877920950
BETA2=4.701142847
CALL XINIT(TH,THD,DEFM,DEFMD,VO,POSO,A,XML,XMU,...
XLL,XMR,E,ZI,PS,CTM,VT,BE,DM,XKV,TE,QL,...
PL,PLIC,REIC)

```

DERIVATIVE

```

*
* COEFFICIENTS FOR BOTH LARGE AND SMALL MOTION ACCELERATIONS
* AND THE RIGHT-HAND SIDES ARE COMPUTED IN THE FOLLOWING
* SUBROUTINES. ALSO THE HYDRAULIC DYNAMICS ARE INCLUDED
* IN THE MAIN PROGRAM.

```

```

*
NOSORT
*
*       HYDRAULIC DYNAMICS
*
      XIINP(1)=DEIC(1)
      IF(PL(1).GT.PS(1)) GO TO 2
      GO TO 3
2     PL(1)=PS(1)
3     QERR1(1)=(XIINP(1)*XKV(1)*DSQRT(PH(1)-PL(1)))-(DM(1)*THD(1))
      QERR(1)=QERR1(1)/CTM(1)
      DIFF(1)=QERR(1)-PL(1)
      FACTOR(1)=VT(1)/(4.0D0*BE(1)*CTM(1))
      DIFF1(1)=DIFF(1)
SORT
      PL1=INTGRL(PLIC,DIFF1,1)
NOSORT
      PL(1)=PL1(1)/FACTOR(1)
      TORQUE(1)=TE(1)*PL(1)*DM(1)
*
*       MATRIX AND VECTOR FORMULATION SUBROUTINE
*
      CALL FORM(W,WTH,WD,DL1,DL1D,XIL,XIR,ARTH,WRDD,ARRDD,U,UD,...
      XMQOP,G,H11,H21,DL11,H41,XK11,A,XMU,XML,XLL,TH,THD,...
      DEFM,DEFMD,E,ZI,XMR,XXM)
*
*       COEFFICIENT OF LARGE MOTION ACCELERATION IN LARGE MOTION DYNAMICS
*       EQUATION SUBROUTINE
*
      CALL XLMMQQ(XMQQ,U,XMQOP,DL1,WTH,ARTH,XIL,XIR,A,XMU,TH,DEFM)
*
*       COEFFICIENTS OF SMALL MOTION ACCELERATIONS IN LARGE MOTION DYNAMICS
*       EQUATION SUBROUTINE
*
      CALL XLMMQN(XMQN,A,XMU,XML,XLL,XXM,DEFM)
*
*       RIGHT-HAND SIDE FOR LARGE MOTION DYNAMICS EQUATION SUBROUTINE
*
      CALL XLMFO(FQ,U,XMQOP,DL1,WTH,ARTH,XIL,XIR,UD,H11,G,H21,WRDD,...
      DL1D,WD,ARRDD,H41,TH,THD,DEFM,DEFMD,A,XMU,XML,XLL,...
      TORQUE,FTT)
*
*       LINK STIFFNESS MATRIX SUBROUTINE
*
      CALL SMKN(XKN,XK11,XMQOP,A,XMU,THD)
*
*       COEFFICIENTS OF LARGE MOTION ACCELERATION IN SMALL MOTION
*       DYNAMICS EQUATIONS SUBROUTINE
*
      CALL SMMNQ(XMNQ,DL1,WTH,XIL,DL11,W,TH,DEFM,A,XMU,...
      XLL)
*
*       RIGHT-HAND SIDE OF SMALL MOTION DYNAMICS EQUATIONS SUBROUTINE
*
      CALL SMFN(FN,H21,W,G,WRDD,DL1,XIL,DL11,WD,DL1D,H41,TH,...
      THD,DEFM,DEFMD)
*
*       COEFFICIENTS OF SMALL MOTION ACCELERATIONS IN SMALL MOTION DYNAMICS
*       EQUATIONS SUBROUTINE
*
      CALL SMMNN(XMNN,XMQOP,XML,A,XMU)
*
*       ACCELERATION COEFFICIENTS MATRIX AND RIGHT-HAND SIDE VECTOR
*       FORMULATION SUBROUTINE
*
      CALL BIGFOR(BIGM,BIGF,XMQQ,XMQN,FQ,XMNQ,XMNN,XKN,FN,U,DEFMD)
*
*       LINEAR EQUATION SOLVER FOR ACCELERATIONS SUBROUTINE
*
      CALL XLEQ(BIGM,BIGF,SOL)

```

```

*
*
* INTEGRATE ACCELERATIONS AND THEN VELOCITY TO GET LARGE MOTION
* ANGULAR POSITION AND SMALL MOTION, LOCAL COORDINATE, TIP POSITION
*
      DO 5 I=1,2
      SOL1(I)=SOL(I)
5     CONTINUE
SORT  VEL=INTGRL(VO,SOL1,2)
NOSORT
      THD(1)=VEL(1)
      DEFMD(1)=VEL(2)
      DO 10 I=1,2
      VEL1(I)=VEL(I)
10    CONTINUE
SORT  POS=INTGRL(POSO,VEL1,2)
NOSORT
      TH(1)=POS(1)
      ANG=TH(1)
      CUR=XIINP(1)
      DEFM(1)=POS(2)
      AC1=SOL1(1)
      AC2=SOL1(2)
      VE1=VEL(1)
      VE2=VEL(2)
      PO1=POS(1)
      PO2=POS(2)
*
* ANGULAR ACCELERATION, VELOCITY, ANGLE.
*
      TAG2=AC1+AC2/0.9985D0
      TAG1=VE1+VE2/0.9985D0
      TAG =PO1 +PO2/0.9985D0
*
* COEFFICIENT OF THE CONTROL ALGORITHM
* CALL CCO(XMOQ,XMQN,XMNN,XMNQ,FTT,FN,XKN,...
* DEFM,CTB,FCO, DEFMD)
*
* CALCULATE THE REQUIRED TORQUE
*
* CALL REQTO(RETO,CTB,TAG1,TAG,FCO,GKV,GKP,DEA)
*
* INVERSE HYDRAULIC DYNAMIC
*
* CALCULATE THE REQUIRED CURRENT
*
* CALL REC(RETO,PL,TE,DM,VT,THD,PS,CTM,XKV,REIC,BE)
* TORK=DETO(1)
* CU=DEIC(1)
*
* TERMINAL
* METHOD ADAMS
* PRINT 12.0E-3, TAG ,TORK ,CU
* SAVE 6.0E-3,TAG
* CONTROL FINTIM=5.000 ,DELT=0.006
* END
* PARAM GKV=4.0 ,GKP=4.0
* END
* PARAM GKV=8.0 ,GKP=16.0
* GRAPH (G1,DE=TEK618) TIME(UN=SEC),TORK
* LABEL (G1) LOAD=2.1151 KG
* GRAPH (G2,DE=TEK618) TIME(UN=SEC),TAG
* LABEL (G2) LOAD=2.1151 KG
* GRAPH (G3,DE=TEK618) TIME,CU
* LABEL (G3) LOAD=2.1151 KG
* GRAPH (G4,DE=TEK618) TIME,TAG1
* LABEL (G4) LOAD=2.1151 KG
* GRAPH (G5,DE=TEK618) TIME,TAG2
* LABEL (G5) LOAD=2.1151 KG

```

END  
STOP

\* LISTING OF SUBROUTINES

\*  
\* FORTRAN  
\*  
\*  
\* .....

\* SUBROUTINE XINIT(TH,THD,DEFM,DEFMD,VO,POSO,A,ML,MU,LL,  
#MR,E,ZI,PS,CTM,VT,BE,DM,KV,TE,QL,PL,PLIC,REIC )  
REAL\*8 VO(2),POSO(2),ML,MU,LL,MR,TH,THD,DEFM,DEFMD,  
#A,E,ZI,ITORQ,PS,CTM,VT,BE,DM,KV,TE,QL,PL,PLIC,  
#C1,C2,A1P,A2P,BETA1,BETA2,REIC,  
#DEPL,DEQ,DI,DEFP,DEIC1,DEIC2

\*  
\* ITORQ= 44.554950510000000  
\* DM=6.2271D-05  
\* TE=.900000000000000  
\* PL=ITORQ/(DM\*TE)  
\* PLIC=PL  
\* CTM=3.7064772D-13  
\* QL=CTM\*PL  
\* KV=2.402963D-09  
\* PS=1.37888D+07  
\* VT=3.05127D-04  
\* BE=690.D6  
\* A=6.17795D-04  
\* ML=2.115100000000000  
\* MU=7861.050000000000000  
\* LL=0.998500000000000  
\* MR=9.000114510000000  
\* E=2.0D11  
\* ZI=4.065D-10  
\* VO(1)=0.000000000000000  
\* VO(2)=0.000000000000000  
\* POSO(1)=0.000000000000000  
\* POSO(2)=-.146064149000000  
\* TH=POSO(1)  
\* THD=VO(1)  
\* DEFM=POSO(2)  
\* DEFMD=VO(2)  
\* REIC=4.0  
\* RETURN  
\* END

\* .....

DOUBLE PRECISION FUNCTION ONE(X)  
REAL\*8 C1,C2,A1P,A2P,BETA1,BETA2  
COMMON/FCDATA/C1,C2,A1P,A2P,BETA1,BETA2

ONE= C1\*(A1P\*(COS(BETA1\*X)+COSH  
# (BETA1\*X))+{SIN(BETA1\*X)+SINH(BETA1\*X)})+  
# C2\*(A2P\*(COS(BETA2\*X)+COSH(BETA2\*X))+  
# {SIN(BETA2\*X)+SINH(BETA2\*X)})

RETURN  
END

C

DOUBLE PRECISION FUNCTION TWO(X)  
REAL\*8 C1,C2,A1P,A2P,BETA1,BETA2  
COMMON/FCDATA/C1,C2,A1P,A2P,BETA1,BETA2

TWO= (C1\*(A1P\*(COS(BETA1\*X)+COSH  
# (BETA1\*X))+{SIN(BETA1\*X)+SINH(BETA1\*X)})+  
# C2\*(A2P\*(COS(BETA2\*X)+COSH(BETA2\*X))+  
# {SIN(BETA2\*X)+SINH(BETA2\*X)}))\*\*2

RETURN  
END

DOUBLE PRECISION FUNCTION SIX(X)  
REAL\*8 C1,C2,A1P,A2P,BETA1,BETA2  
COMMON/FCDATA/C1,C2,A1P,A2P,BETA1,BETA2

```

SIX=          .9985*(C1*(A1P*(COS(BETA1*X)+COSH
#             (BETA1*X))+{SIN(BETA1*X)+SINH(BETA1*X)})+
#             C2*(A2P*(COS(BETA2*X)+COSH(BETA2*X))+
#             {SIN(BETA2*X)+SINH(BETA2*X)})))+
#             X*(C1*(A1P*(COS(BETA1*X)+COSH
#             (BETA1*X))+{SIN(BETA1*X)+SINH(BETA1*X)})+
#             C2*(A2P*(COS(BETA2*X)+COSH(BETA2*X))+
#             {SIN(BETA2*X)+SINH(BETA2*X)}))
RETURN
END

```

```

DOUBLE PRECISION FUNCTION EIGHT(X)
REAL*8 C1,C2, A1P,A2P,BETA1,BETA2
COMMON/FCDATA/C1,C2, A1P,A2P,BETA1,BETA2

```

```

EIGHT=        (C1*BETA1*BETA1*(A1P*(-COS
#             (BETA1*X)+COSH(BETA1*X))+{-SIN(BETA1*X)+SINH(BETA1*X)})))+
#             C2*BETA2*BETA2*(A2P*(-COS(BETA2*X)+COSH(BETA2*X))+
#             {-SIN(BETA2*X)+SINH(BETA2*X)}))**2
RETURN
END

```

\* .....  
\* .....  
\* .....

```

SUBROUTINE FORM(W,WTH,WD,DL1,DL1D,XIL,XIR,ARTH,WRDD,ARRDD,U,UD,
#XMQQP,G,H11,H21,DL11,H41,XK11,A,MU,ML,LL,TH,THD,DEFM,DEFMD,
#E,ZI,MR,MX)
REAL*8 W(3,3),WTH(3,3),WD(3,3),DL1(3,3),DL1D(3,3),XIL(3,3)
REAL*8 XIR(3,3),ARTH(3,3),WRDD(3,3),ARRDD(3,3),U,UD
REAL*8 XMQQP,G(3,1),H11(1,3),H21(1,3),DL11(3,3)
REAL*8 H41(1,3),XK11,MU,ML,LL,MR,MX,TH
REAL*8 THD,DEFM,DEFMD,A,E,ZI
REAL*8 C1,A1P,BETA1
REAL*8 ONE,TWO,EIGHT,Y
EXTERNAL ONE,TWO,EIGHT
W(1,1)=1.0000000000000000
W(1,2)=0.0000000000000000
W(1,3)=0.0000000000000000
W(2,1)=LL*DCOS(TH)
W(2,2)=DCOS(TH)
W(2,3)=-DSIN(TH)
W(3,1)=LL*DSIN(TH)
W(3,2)=DSIN(TH)
W(3,3)=DCOS(TH)
WTH(1,1)=0.0000000000000000
WTH(1,2)=0.0000000000000000
WTH(1,3)=0.0000000000000000
WTH(2,1)=-LL*DSIN(TH)
WTH(2,2)=-DSIN(TH)
WTH(2,3)=-DCOS(TH)
WTH(3,1)=LL*DCOS(TH)
WTH(3,2)=DCOS(TH)
WTH(3,3)=-DSIN(TH)
WD(1,1)=0.0000000000000000
WD(1,2)=0.0000000000000000
WD(1,3)=0.0000000000000000
WD(2,1)=-LL*DSIN(TH)*THD
WD(2,2)=-DSIN(TH)*THD
WD(2,3)=-DCOS(TH)*THD
WD(3,1)=LL*DCOS(TH)*THD
WD(3,2)=DCOS(TH)*THD
WD(3,3)=-DSIN(TH)*THD
DL1(1,1)=1.0000000000000000
DL1(1,2)=0.0000000000000000
DL1(1,3)=0.0000000000000000
DL1(2,1)=0.0000000000000000
DL1(2,2)=1.0000000000000000
DL1(2,3)=0.0000000000000000
DL1(3,1)=DEFM

```

```

DL1(3,2)=0.0000000000000000
DL1(3,3)=1.0000000000000000
DL1D(1,1)=0.0000000000000000
DL1D(1,2)=0.0000000000000000
DL1D(1,3)=0.0000000000000000
DL1D(2,1)=0.0000000000000000
DL1D(2,2)=0.0000000000000000
DL1D(2,3)=0.0000000000000000
DL1D(3,1)=DEFMD
DL1D(3,2)=0.0000000000000000
DL1D(3,3)=0.0000000000000000
XIL(1,1)=ML
XIL(1,2)=0.0167854590000000
XIL(1,3)=0.0000000000000000
XIL(2,1)=0.0167854590000000
XIL(2,2)=1.77679D-04
XIL(2,3)=0.0000000000000000
XIL(3,1)=0.0000000000000000
XIL(3,2)=0.0000000000000000
XIL(3,3)=2.986791D-03
MX=.0167854590000000
XIR(1,1)=MR
XIR(1,2)=0.0000000000000000
XIR(1,3)=0.0000000000000000
XIR(2,1)=0.0000000000000000
XIR(2,2)=.0274671300000000
XIR(2,3)=0.0000000000000000
XIR(3,1)=0.0000000000000000
XIR(3,2)=0.0000000000000000
XIR(3,3)=.0274671300000000
ARTH(1,1)=0.0000000000000000
ARTH(1,2)=0.0000000000000000
ARTH(1,3)=0.0000000000000000
ARTH(2,1)=0.0000000000000000
ARTH(2,2)=-DSIN(TH)
ARTH(2,3)=-DCOS(TH)
ARTH(3,1)=0.0000000000000000
ARTH(3,2)=DCOS(TH)
ARTH(3,3)=-DSIN(TH)
WRDD(1,1)=0.0000000000000000
WRDD(1,2)=0.0000000000000000
WRDD(1,3)=0.0000000000000000
WRDD(2,1)=-LL*DCOS(TH)*(THD**2)
WRDD(2,2)=-DCOS(TH)*(THD**2)
WRDD(2,3)=DSIN(TH)*(THD**2)
WRDD(3,1)=-LL*DSIN(TH)*(THD**2)
WRDD(3,2)=-DSIN(TH)*(THD**2)
WRDD(3,3)=-DCOS(TH)*(THD**2)
ARRDD(1,1)=0.0000000000000000
ARRDD(1,2)=0.0000000000000000
ARRDD(1,3)=0.0000000000000000
ARRDD(2,1)=0.0000000000000000
ARRDD(2,2)=-DCOS(TH)*(THD**2)
ARRDD(2,3)=DSIN(TH)*(THD**2)
ARRDD(3,1)=0.0000000000000000
ARRDD(3,2)=-DSIN(TH)*(THD**2)
ARRDD(3,3)=-DCOS(TH)*(THD**2)
U      =DEFM
UD     =DEFMD
CALL DQG4(-LL,0.DO,TWO,Y)
XMQQP =Y
G(1,1)=0.0000000000000000
G(2,1)=0.0000000000000000
G(3,1)=-9.8066000000000000
H11(1,1)=4.8565190000000000
H11(1,2)=-2.4282586930000000
H11(1,3)=0.0000000000000000
H21(1,1)=0.0000000000000000
H21(1,2)=0.0000000000000000
CALL DQG4(-LL,-0.DO,ONE ,Y)

```

```

H21(1,3)=A*MU*Y
DO 50 I=1,3
DO 60 J=1,3
DL11(I,J)=0.0000000000000000
60 CONTINUE
50 CONTINUE
DL11(3,1)=1.0000000000000000
H41(1,1)=ML
H41(1,2)=0.0000000000000000
H41(1,3)=.01678545900000000000
CALL DQG4(-LL,0.DO,EIGHT,Y)
XK11 =Y*E*ZI
RETURN
END

```

\*  
\*  
\*

```

SUBROUTINE XLMMQO(MOO,U,XMQOP,DL1,WTH,ARTH,XIL,XIR,A,MU,TH,DEFM)
REAL*8 MOO,UT,P,DL1T(3,3),WTHT(3,3),ARTHT(3,3),P1(3,3)
REAL*8 P2(3,3),P3(3,3),P4(3,3),P5(3,3),P6(3,3),P7(3,3),MU
REAL*8 U,XMQOP,DL1(3,3),WTH(3,3),ARTH(3,3),XIL(3,3)
REAL*8 XIR(3,3),A,TH,DEFM,SP,TP
M=2
L=1
N=3
MOO=0.0000000000000000
CALL TRANS(U,UT,L,L)
CALL MATMUL(UT,XMQOP,L,L,L,P)
CALL MATMUL(P,U,L,L,L,SP)
CALL TRANS(DL1,DL1T,N,N)
CALL TRANS(ARTH,ARTHT,N,N)
CALL TRANS(WTH,WTHT,N,N)
CALL MATMUL(WTH,DL1,N,N,N,P1)
CALL MATMUL(P1,XIL,N,N,N,P2)
CALL MATMUL(P2,DL1T,N,N,N,P3)
CALL MATMUL(P3,WTHT,N,N,N,P4)
CALL MATMUL(P4,ARTH,XIR,N,N,N,P5)
CALL MATMUL(P5,ARTHT,N,N,N,P6)
CALL MATADD(P4,P6,N,N,P7)
CALL TRACE(P7,N,TP)
MOO=((1./3.)*A*MU) + (A*MU*SP) + TP
RETURN
END

```

\*  
\*  
\*

```

SUBROUTINE XLMMQN(XMQN,A,MU,ML,LL,MX,DEFM)
REAL*8 XMQN,MU,ML,LL,MX,A,DEFM
REAL*8 C1,A1P,BETA1,Y,SIX,C2,A2P,BETA2
EXTERNAL SIX
CALL DQG4(-LL,0.DO,SIX,Y)
XMQN =(A*MU*Y)+(ML*LL)+MX
RETURN
END

```

\*  
\*  
\*

```

SUBROUTINE XLMFO(FQ,U,XMQOP,DL1,WTH,ARTH,XIL,XIR,UD,H11,G,H21,
#WRDD,DL1D,WD,ARRDD,H41,TH,THD,DEFM,DEFMD,A,MU,ML,LL,
#TORQUE,FTT)
REAL*8 FQP,P,P1(1,3),P2(1,3),P3(1,3),P4(3,3),P5(3,3)
REAL*8 P6(3,3),P7(3,3),P8(3,3),P9(3,3),P10(3,3),P11(1,3),P12(1,3)
REAL*8 FPFH(3,3),FHP(3,3),FPT(3,3),DL1DT(3,3),WDT(3,3),ARRDDT(3,3)
REAL*8 UT,DL1T(3,3),WRDDT(3,3),FPF(3,3),FPS(3,3),WTHT(3,3)
REAL*8 U,XMQOP,DL1(3,3),WTH(3,3),ARTH(3,3),XIL(3,3)
REAL*8 XIR(3,3),UD,H11(1,3),G(3,1),H21(1,3),WRDD(3,3)
REAL*8 DL1D(3,3),WD(3,3),ARRDD(3,3),H41(1,3),MU,ML,LL
REAL*8 A,TORQUE,FQ,TH,THD,DEFM,DEFMD
REAL*8 FP,SP,TP,TFP,FTHP,FTT
M=2

```

```

L=1
N=3
CALL TRANS(U,UT,L,L)
FQP=XMQOP *THD
CALL MATMUL(UT,FQP,L,L,L,P)
CALL MATMUL(P,UD,L,L,L,FP)
CALL TRANS(WTH,WTHT,N,N)
CALL MATMUL(H11,WTHT,L,N,N,P1)
CALL MATMUL(P1,G,L,N,L,SP)
CALL MATMUL(UT,H21,L,M,N,P2)
CALL MATMUL(P2,WTHT,L,N,N,P3)
CALL MATMUL(P3,G,L,N,L,TP)
CALL TRANS(DL1,DL1T,N,N)
CALL TRANS(WRDD,WRDDT,N,N)
CALL MATMUL(WTH,DL1,N,N,N,P4)
CALL MATMUL(P4,XIL,N,N,N,P5)
CALL MATMUL(P5,DL1T,N,N,N,P6)
CALL MATMUL(P6,WRDDT,N,N,N,FPF)
CALL TRANS(DL1D,DL1DT,N,N)
CALL TRANS(WD,WDT,N,N)
CALL MATMUL(WTH,DL1,N,N,N,P7)
CALL MATMUL(P7,XIL,N,N,N,P8)
CALL MATMUL(P8,DL1DT,N,N,N,P9)
CALL MATMUL(P9,WDT,N,N,N,FPS)
CALL TRANS(ARRDD,ARRDDT,N,N)
CALL MATMUL(ARTH,XIR,N,N,N,P10)
CALL MATMUL(P10,ARRDDT,N,N,N,FPT)
DO 30 I=1,3
DO 40 J=1,3
FPS(I,J)=FPS(I,J)*2.
40 CONTINUE
30 CONTINUE
CALL MATADD(FPF,FPS,N,N,FPFH)
CALL MATADD(FPFH,FPT,N,N,FHP)
CALL TRACE(FHP,N,TFP)
CALL MATMUL(H41,DL1T,L,N,N,P11)
CALL MATMUL(P11,WTHT,L,N,N,P12)
CALL MATMUL(P12,G,L,N,L,FTHP)
FTT=(-2.*A*MU*FP) + SP + TP - TFP + FTHP
FQ=FTT+TORQUE
RETURN
END

```

\*  
\*  
\*

```

SUBROUTINE SMKN(XKN,XK11,XMQOP,A,MU,THD)
REAL*8 XKN,KNP,XMQOP,XK11,A,THD,MU
KNP=XMQOP*(-A)*MU*(THD**2)
XKN=KNP+XK11
RETURN
END

```

\*  
\*  
\*

```

SUBROUTINE SMMNQ(XMNO,DL1,WTH,XIL,DL11,W,TH,DEFM,A,MU,
#LL)
REAL*8 XMNO,DL11T(3,3),WT(3,3),P1(3,3),P2(3,3)
REAL*8 P3(3,3),P4(3,3),DL1(3,3),WTH(3,3),XIL(3,3)
REAL*8 W(3,3),DL11(3,3),TH,DEFM,A,MU,LL
REAL*8 C1,A1P,BETA1
REAL*8 SIX,Y,C2,A2P,BETA2
EXTERNAL SIX
M=2
L=1
N=3
CALL TRANS(DL11,DL11T,N,N)
CALL TRANS(W,WT,N,N)
CALL MATMUL(WTH,DL1,N,N,N,P1)
CALL MATMUL(P1,XIL,N,N,N,P2)
CALL MATMUL(P2,DL11T,N,N,N,P3)

```

```

CALL MATMUL(P3,WT,N,N,N,P4)
CALL TRACE(P4,N,TFP1)
CALL DOG4(-LL,0.DO,SIX ,Y)
XMNO =TFP1 + (Y*A*MU)
RETURN
END

```

\*  
\*  
\*

```

.....
SUBROUTINE SMFN(FN,H21,W,G,WRDD,DL1,XIL,DL11,      WD,DL1D,H41,TH,
#THD,DEFM,DEFMD)
REAL*8 FN,P1(1,3),P2(3,3),P3(3,3),P4(3,3),P5(3,3),P6(3,3)
REAL*8 P7(3,3),P8(3,3),P9(3,3)
REAL*8 P14(1,3),P15(1,3),TP,FP,SP
REAL*8 FN1(3,3),G(3,1),H21(1,3),WRDD(3,3),DL1D(3,3)
REAL*8 WD(3,3),H41(1,3),XIL(3,3),W(3,3),DL11(3,3)
REAL*8 DL1(3,3),DL11T(3,3),WT(3,3)
REAL*8 TH,THD,DEFM,DEFMD,TFN1,FN3
M=2
L=1
N=3
CALL TRANS(W,WT,N,N)
CALL MATMUL(H21,WT,L,N,N,P1)
CALL MATMUL(P1,G,L,N,L,FP)
CALL TRANS(DL11,DL11T,N,N)
CALL MATMUL(WRDD,DL1,N,N,N,P2)
CALL MATMUL(P2,XIL,N,N,N,P3)
CALL MATMUL(P3,DL11T,N,N,N,P4)
CALL MATMUL(P4,WT,N,N,N,P5)
CALL MATMUL(WD,DL1D,N,N,N,P6)
CALL MATMUL(P6,XIL,N,N,N,P7)
CALL MATMUL(P7,DL11T,N,N,N,P8)
CALL MATMUL(P8,WT,N,N,N,P9)
DO 10 I=1,3
DO 20 J=1,3
P9(I,J)= P9(I,J)*2.
20 CONTINUE
10 CONTINUE
CALL MATADD(P5,P9,N,N,FN1)
CALL TRACE(FN1,N,TFN1)
SP =TFN1
CALL MATMUL(H41,DL11T,L,N,N,P14)
CALL MATMUL(P14,WT,L,N,N,P15)
CALL MATMUL(P15,G,L,N,L,FN3)
TP =FN3
FN=FP -SP + TP
RETURN
END

```

\*  
\*  
\*

```

.....
SUBROUTINE SMMNN(XMNN,XMQQP,ML,A,MU      )
REAL*8 XMNN,XMQQP ,ML,MU,A
XMNN =ML
XMNN =XMNN + XMQQP *A*MU
RETURN
END

```

\*  
\*  
\*

```

.....
SUBROUTINE MATMUL(A,B,M,L,N,C)
REAL*8 A(M,L),B(L,N),C(M,N)
DO 10 I=1,M
DO 20 J=1,N
C(I,J)=0.0
DO 30 INDEX=1,L
C(I,J)=C(I,J) + A(I,INDEX)*B(INDEX,J)
30 CONTINUE
20 CONTINUE
10 CONTINUE

```

```

        RETURN
        END
*
* .....
*
        SUBROUTINE TRANS(A,B,M,L)
        REAL*8 A(M,L),B(L,M)
        DO 10 I=1,M
        DO 20 J=1,L
        B(J,I)=A(I,J)
20    CONTINUE
10    CONTINUE
        RETURN
        END
*
* .....
*
        SUBROUTINE TRACE(A,M,TRAC)
        REAL*8 A(M,M)
        TRAC=0.0
        DO 10 I=1,M
        TRAC=TRAC + A(I,I)
10    CONTINUE
        RETURN
        END
*
*
* MATRIX ADDITION SUBROUTINE
*
        SUBROUTINE MATADD(A,B,M,L,C)
        REAL*8 A(M,L),B(M,L),C(M,L)
        DO 10 I=1,M
        DO 20 J=1,L
        C(I,J)=A(I,J) + B(I,J)
20    CONTINUE
10    CONTINUE
        RETURN
        END
*
* .....
*
        SUBROUTINE BIGFOR(BIGM,BIGF,MOQ,XMQN,FQ,XMNQ,XMNN,XKN,FN,U,DEFMD)
        REAL*8 BIGM(2,2),BIGF(2,1),XMQN,XMNQ,XMNN,XKN
        REAL*8 FN,U,MOQ,P,FQ,DEFMD
        M=2
        L=1
        BIGM(1,1)=MOQ
        BIGM(1,2)=XMQN
        BIGM(2,1)=XMNQ
        BIGM(2,2)=XMNN
        BIGF(1,1)=FQ
        CALL MATMUL(XKN,U,L,L,L,P)
        BIGF(2,1)=FN -P
        RETURN
        END
*
* .....
*
        SUBROUTINE XLEQ(BIGM,BIGF,SOL)
        REAL*8 BIGM(2,2),BIGF(2,1),SOL(2),WKAREA(18)
        M=1
        N=2
        CALL LEQT2F (BIGM,M,N,N,BIGF,M,WKAREA,IER)
        DO 10 I=1,2
        SOL(I)=BIGF(I,1)
10    CONTINUE
        RETURN
        END
*
*
* SUBROUTINE LEQT2F (IMSL)

```

```

*
* PURPOSE - LINEAR EQUATION SOLUTION - FULL STORAGE
*          MODE - HIGH ACCURACY SOLUTION
*
* USAGE - CALL LEQT2F (A,M,N,IA,B, IDGT,WKAREA, IER)
*
* ARGUMENTS
*   A - INPUT MATRIX OF DIMENSION N BY N CONTAINING
*       THE COEFFICIENT MATRIX OF THE EQUATION
*       AX = B.
*   M - NUMBER OF RIGHT-HAND SIDES. (INPUT)
*   N - ORDER OF A AND NUMBER OF ROWS IN B. (INPUT)
*   IA - ROW DIMENSION OF A AND B EXACTLY AS SPECIFIED
*        IN THE DIMENSION STATEMENT IN THE CALLING
*        PROGRAM. (INPUT)
*   B - INPUT MATRIX OF DIMENSION N BY M CONTAINING
*       THE RIGHT-HAND SIDES OF THE EQUATION AX = B.
*       ON OUTPUT, THE N BY M MATRIX OF SOLUTIONS
*       REPLACES B.
*   IDGT - INPUT OPTION.
*          IF IDGT IS GREATER THAN 0, THE ELEMENTS OF
*          A AND B ARE ASSUMED TO BE CORRECT TO IDGT
*          DECIMAL DIGITS AND THE ROUTINE PERFORMS
*          AN ACCURACY TEST.
*          IF IDGT EQUALS 0, THE ACCURACY TEST IS
*          BYPASSED.
*          ON OUTPUT, IDGT CONTAINS THE APPROXIMATE
*          NUMBER OF DIGITS IN THE ANSWER WHICH
*          WERE UNCHANGED AFTER IMPROVEMENT.
*   WKAREA - WORK AREA OF DIMENSION GREATER THAN OR EQUAL
*            TO N**2+3N.
*   IER - ERROR PARAMETER. (OUTPUT)
*        WARNING ERROR
*        IER = 34 INDICATES THAT THE ACCURACY TEST
*        FAILED. THE COMPUTED SOLUTION MAY BE IN
*        ERROR BY MORE THAN CAN BE ACCOUNTED FOR
*        BY THE UNCERTAINTY OF THE DATA. THIS
*        WARNING CAN BE PRODUCED ONLY IF IDGT IS
*        GREATER THAN 0 ON INPUT. (SEE THE
*        CHAPTER L PRELUDE FOR FURTHER DISCUSSION.)
*        TERMINAL ERROR
*        IER = 129 INDICATES THAT THE MATRIX IS
*        ALGORITHMICALLY SINGULAR. (SEE THE
*        CHAPTER L PRELUDE).
*        IER = 131 INDICATES THAT THE MATRIX IS TOO
*        ILL-CONDITIONED FOR ITERATIVE IMPROVEMENT
*        TO BE EFFECTIVE.
* REQD. IMSL ROUTINES - SINGLE/LUDATN,LUELMN,LUREFN,UERTST,UGETIO
*                      - DOUBLE/LUDATN,LUELMN,LUREFN,UERTST,UGETIO,
*                      VXADD,VXMUL,VXSTO
* .....
* SUBROUTINE LEQT2F (A,M,N,IA,B, IDGT,WKAREA, IER)
*
* DIMENSION A(IA,1),B(IA,1),WKAREA(1)
* DOUBLE PRECISION A,B,WKAREA,D1,D2,WA
*          FIRST EXECUTABLE STATEMENT
*          INITIALIZE IER
*
* IER=0
* JER=0
* J = N*N+1
* K = J+N
* MM = K+N
* KK = 0
* MM1 = MM-1
* JJ=1
* DO 5 L=1,N
*   DO 5 I=1,N
*     WKAREA(JJ)=A(I,L)
*     JJ=JJ+1
* 5 CONTINUE
*
* DECOMPOSE A

```



```

REAL*8 B33,B44,F11,F22,DEFMD,F33
B11=XMQQ/0.9985
B22=XMON-B11
B33=XMNQ/0.9985
B44=XMNN-B33
CTA=B22/B44
CTB=XMQQ-CTA*XMNQ
F11=CTA*FN
F22=(CTA*XKN)*DEFM
F33=(CTA*0.00)*DEFMD
FCO=F11-F22-FTT -F33
RETURN
END

```

\*.....\*

```

SUBROUTINE REQTO(RETO,CTB,TAG1,TAG,FCO,GKV,GKP,DEA)
REAL*8 DETO1,DETO2,RETO,GKV,GKP,DEA,TAG1,TAG,FCO,CTB
DETO1=(-GKV*TAG1)+GKP*(DEA-TAG)
DETO2=CTB*DETO1
RETO=DETO2+FCO
RETURN
END

```

\*.....\*

```

SUBROUTINE REC(RETO,PL,TE,DM,VT,THD,PS,CTM,XKV,DEIC,BE)
REAL*8 RETO,PL,TE,DM,VT,THD,PS,CTM,XKV,REIC,BE
REAL*8 DI,DEQ,DEFP,DEIC1,DEIC2
DEPL =DETO /((TE *DM ))
DI =VT *(DEPL -PL )/(4.000*BE *0.00600)
DEQ =DM *THD +CTM *DEPL +DI
DEFP = (PS - DEPL )
IF(DEFP .LT.0.0) GO TO 13
DEIC1=DSQRT(DEFP)
GO TO 14
13 DEFP=-DEFP
DEIC1=DSQRT(DEFP)
14 DEIC2=DEIC1*XKV
REIC =DEQ /((DEIC2 ))
RETURN
END

```

## LIST OF REFERENCES

1. Whitney, D. E., Book, W. J., and Lynch, P. M., "Design and Control Configurations for Industrial and Space Manipulators." Proc. JACC, 1974.
2. Book, W. J., "Feedback Control of Two Beam, Two Joint Systems With Distributed Flexibility," Journal of Dynamic Systems, Measurement and Control, Vol. 97, No. 4, pp. 424-430, Dec. 1975.
3. Sunada, H. H., and Dubowsky, S., "On the Dynamic Analysis and Behavior of Industrial Robotic Manipulators with Elastic Members," ASME Journal of Mechanisms, Transmissions, and Automation in Design, Vol. 105, pp. 42-51, Mar. 1983.
4. Chang, L. W., *Dynamic Analysis of Robotic manipulators with Flexible links*, Ph.D. Thesis, Purdue University, Dec. 1984.
5. Petroka, R. P., *Computer Simulation And Experimental Validation Of A Dynamic Model (Equivalent Rigid Link System) On A Single -Link Flexible Manipulator*, M.S. Thesis, Naval Postgraduate School, Monterey, CA, Oct. 1982.
6. Gannon, K. P., *Modeling And Experimental Validation Of A Single - Link Flexible Manipulator*, M.S. Thesis, Naval Postgraduate School, Monterey, CA, Dec. 1986.
7. Cannon, R. H. and Schmitz, E., "Initial Experiments on the End Point Control of a Flexible One- Link Robot Flexible," The International Journal for Robotics Research, Vol. 3, No. 3, pp. 62-75, Fall, 1984.
8. MOOG INC. MOOG Series 760 Two-Stage Flow Control Servovalve Catalog, MOOG INC., EAST Aurora, N.Y.
9. Merrit, H. E., "Hydraulic Controls Systems", Wiley, N.Y., 1967.

## INITIAL DISTRIBUTION LIST

		No. Copies
1.	Defense Technical Information Center Cameron Station Alexandria, VA 22304-6145	2
2.	Library, Code 0142 Naval Postgraduate School Monterey, CA 93943-5002	2
3.	Department Chairman, Code 69 Dept. of Mechanical Engineering Naval Postgraduate School Monterey, CA 93943-5000	1
4.	Prof. L. W. Chang, Code 69Ck Dept. of Mechanical Engineering Naval Postgraduate School Monterey, CA 93943-5000	6
5.	Dr. Kil Soo Kim, Code 69Ki Dept. of Mechanical Engineering Naval Postgraduate School Monterey, CA 93943-5000	1
6.	Park, Ki Soon Busong Dong 534, I Ri City, Jon Ra Buk Do, Republic of Korea	7
7.	Air Force Central Library Sindaeban Dong, Kwanak Gu, Seoul, Republic of Korea	1
8.	Library of Air Force Academy Chongwon Gun, Chung Cheong Buk Do, Republic of Korea	1
9.	Department of Mechanical Engineering Air Force Academy Chongwon Gun, Chung Cheong Buk Do, Republic of Korea	3
10.	Prof. David Smith, Code 69Sm Dept. of Mechanical Engineering Naval Postgraduate School Monterey, CA 93943-5000	1

11. Chief of Naval Operations  
OP-02  
Navy Department  
Washington, D.C. 20350-2000 1
12. Chief of Naval Operations  
OP-03  
Navy Department  
Washington, D.C. 20350-2000 1
13. Chief of Naval Operations  
OP-05  
Navy Department  
Washington, D.C. 20350-2000 1
14. Dr. Alan L. Meyrowitz, Code 433  
ONR  
800 N. Quincy St.  
Arlington, VA 22217 1

END  
DATE  
FILMED  
JAN  
1988